

DTIC FILE COPY

MEMORANDUM REPORT BRL-MR-3877

BRL

AD-A229 713

AERODYNAMIC CHARACTERISTICS OF
CALIBER .22 LONG RIFLE MATCH AMMUNITION

ROBERT L. McCOY

NOVEMBER 1990

DTIC
ELECTE
NOV 29 1990
S B D

APPROVED FOR PUBLIC RELEASE; DISTRIBUTION UNLIMITED.

U.S. ARMY LABORATORY COMMAND

BALLISTIC RESEARCH LABORATORY
ABERDEEN PROVING GROUND, MARYLAND

Best Available Copy

NOTICES

Destroy this report when it is no longer needed. DO NOT return it to the originator.

Additional copies of this report may be obtained from the National Technical Information Service, U.S. Department of Commerce, 5285 Port Royal Road, Springfield, VA 22161.

The findings of this report are not to be construed as an official Department of the Army position, unless so designated by other authorized documents.

The use of trade names or manufacturers' names in this report does not constitute indorsement of any commercial product.

Best Available Copy

REPORT DOCUMENTATION PAGE

Form Approved
OMB No. 0704-0188

Public reporting burden for this collection of information is estimated to average 1 hour per response, including the time for reviewing instructions, searching existing data sources, gathering and maintaining the data needed, and completing and reviewing the collection of information. Send comments regarding this burden estimate or any other aspect of this collection of information, including suggestions for reducing this burden, to Washington Headquarters Services, Directorate for Information Operations and Reports, 1215 Jefferson Davis Highway, Suite 1204, Arlington, VA 22202-4302, and to the Office of Management and Budget, Paperwork Reduction Project (0704-0188), Washington, DC 20503.

1. AGENCY USE ONLY (Leave blank) 2. REPORT DATE
November 1990 3. REPORT TYPE AND DATES COVERED
Final, Sep 89 - Jun 90

4. TITLE AND SUBTITLE
Aerodynamic Characteristics of Caliber .22 Long Rifle Match Ammunition 5. FUNDING NUMBERS
1L162618AH80 ✓

6. AUTHOR(S)
Robert L. McCoy

7. PERFORMING ORGANIZATION NAME(S) AND ADDRESS(ES)
8. PERFORMING ORGANIZATION REPORT NUMBER

9. SPONSORING/MONITORING AGENCY NAME(S) AND ADDRESS(ES)
U.S. Army Ballistic Research Laboratory
ATTN: SLCBR-DD-T
Aberdeen Proving Ground, MD 21005-5066 10. SPONSORING/MONITORING AGENCY REPORT NUMBER
BRL-MR-3877

11. SUPPLEMENTARY NOTES

12a. DISTRIBUTION / AVAILABILITY STATEMENT
Approved for public release; distribution is unlimited 12b. DISTRIBUTION CODE

13. ABSTRACT (Maximum 200 words)
Spark photography range tests were conducted in the BRL Aerodynamics Range, for caliber .22 Long Rifle match ammunition fired from Olympic-grade competition rifles. The spark range measurements were used to accurately quantify the effect of wind on the trajectory of caliber .22 match ammunition. The tests included two commercial brands of match ammunition and two Olympic-grade rifles. No significant difference in aeroballistic characteristics due to either rifle or ammunition brand could be found. Keywords: Small arms ammunition; Rifles/ballistic trajectories;

14. SUBJECT TERMS
Caliber .22 Long Rifle
Match Ammunition
Aerodynamic Characteristics; Flight Dynamic Characteristics; Gyroscopic Stability; Wind Sensitivity. (EDC) * 15. NUMBER OF PAGES
68 16. PRICE CODE

17. SECURITY CLASSIFICATION OF REPORT
UNCLASSIFIED 18. SECURITY CLASSIFICATION OF THIS PAGE
UNCLASSIFIED 19. SECURITY CLASSIFICATION OF ABSTRACT
UNCLASSIFIED 20. LIMITATION OF ABSTRACT
SAR

A

INTENTIONALLY LEFT BLANK.

Table of Contents

	<u>Page</u>
List of Figures	v
List of Tables	vii
I. Introduction	1
II. Test Procedure and Material	1
III. Aeroballistic Results	2
1. Flowfield Observations	2
2. Aerodynamic Characteristics	3
a. Drag Force Coefficient	3
b. Overturning Moment Coefficient	5
c. Gyroscopic Stability	5
d. Lift Force Coefficient	6
e. Magnus Moment Coefficient and Pitch Damping Moment Coefficient	6
IV. Flight Dynamic Characteristics	8
V. Wind Sensitivity Results	8
VI. Conclusions	11
References	55
List of Symbols	57
Distribution List	61



Accession For	
NTIS GRA&I	<input checked="" type="checkbox"/>
DTIC TAB	<input type="checkbox"/>
Unannounced	<input type="checkbox"/>
Justification	
By _____	
Distribution/	
Availability Codes	
Dist	Avail and/or Special
A-1	

INTENTIONALLY LEFT BLANK.

List of Figures

<u>Figure</u>		<u>Page</u>
1	Photograph of caliber .22 long rifle match ammunition	12
2	Photograph of the Anschutz prone rifle	13
3	Photograph of the Remington 40-X rifle	14
4	Photograph of the BRL free flight aerodynamics range	15
5	Coordinate system for the BRL aerodynamics range	16
6	Sketch of the Eley Tenex bullet	17
7	Sketch of the Ultra match bullet	18
8	Shadowgraph of RWS R-50 bullet at Mach 0.96	19
9	Shadowgraph of Eley Tenex bullet at Mach 0.95	20
10	Shadowgraph of Eley Tenex bullet at Mach 0.90	21
11	Shadowgraph of Eley Tenex bullet at Mach 0.87	22
12	Shadowgraph of Eley type nose bullet at Mach 1.05	23
13	Shadowgraph of Eley type nose bullet at Mach 1.01	24
14	Shadowgraph of Eley type nose bullet at Mach 0.96	25
15	Shadowgraph of Eley type nose bullet at Mach 0.89	26
16	Shadowgraph of Ultra match bullet at Mach 1.05	27
17	Shadowgraph of Ultra match bullet at Mach 0.99	28
18	Shadowgraph of Ultra match bullet at Mach 0.94	29
19	Shadowgraph of Ultra match bullet at Mach 0.91	30
20	Shadowgraph of Ultra match bullet at Mach 0.85	31
21	Zero-yaw drag force coefficient versus Mach number, Eley Tenex and RWS R-50 bullets	32
22	Zero-yaw drag force coefficient versus Mach number, Eley type nose bullet .	33
23	Zero-yaw drag force coefficient versus Mach number, Ultra match bullet . .	34
24	Overturning moment coefficient versus Mach number, Eley Tenex bullet . .	35
25	Overturning moment coefficient versus Mach number, Eley type nose bullet	36
26	Overturning moment coefficient versus Mach number, Ultra match bullet .	37

List of Figures (Continued)

<u>Figure</u>		<u>Page</u>
27	Launch gyroscopic stability factor versus launch Mach number	38
28	Lift force coefficient versus Mach number	39
29	Magnus moment coefficient versus effective squared yaw	40
30	Pitch damping coefficient versus Mach number	40
31	Effect of a 10 mile/hour wind on the Eley Tenex bullet at 50 metres range .	41
32	Effect of a 20 mile/hour wind on the Eley Tenex bullet at 50 metres range .	42
33	Effect of a 30 mile/hour wind on the Eley Tenex bullet at 50 metres range .	43
34	Simplified ballistic prediction of the wind effect on the Eley Tenex bullet at 50 metres range	44

List of Tables

<u>Table</u>		<u>Page</u>
1	Average Physical Characteristics of Caliber .22 Match Bullets	45
2	Aerodynamic Characteristics of the Eley Tenex Bullet	46
3	Aerodynamic Characteristics of the RWS R-50 Bullet	47
4	Aerodynamic Characteristics of the Eley Type Nose Bullet	48
5	Aerodynamic Characteristics of the Ultra Match Bullet	49
6	Flight Motion Parameters of the Eley Tenex Bullet	50
7	Flight Motion Parameters of the RWS R-50 Bullet	51
8	Flight Motion Parameters of the Eley Type Nose Bullet	52
9	Flight Motion Parameters of the Ultra Match Bullet	53

INTENTIONALLY LEFT BLANK.

I. Introduction

In July 1989, a meeting was held at the U.S. Army Ballistic Research Laboratory (BRL), Aberdeen Proving Ground, Maryland, to discuss possible BRL technical assistance to the U.S. Olympic Shooting Team. In attendance were Dr. John Frasier, Director of BRL, Mr. R. L. McCoy of the Launch and Flight Division, BRL, Dr. Henry D. Cross, III, Chairman of the U.S. Shooting Team, Mr. Ray P. Carter of the U.S. Shooting Team, and Ms. Marsha Beasley, National Women's Champion smallbore shooter. Dr. Cross requested assistance from the BRL in defining the effect of wind on the performance of caliber .22 Long Rifle match ammunition used in Olympic competition. The result of the meeting was a decision to conduct a limited firing program of caliber .22 match ammunition in the BRL Aerodynamics Range.¹

The two commercial brands of caliber .22 match ammunition in common use by U.S. Olympic shooters are the British Eley Tenex and the West German RWS R-50. In order to develop a U.S. caliber .22 match round that competes successfully with the British and West German products, the U.S. Shooting Team is currently sponsoring the Ultra Match Project, headed by Mr. Steven Chernicky of Bonsall, California. The firing program in the BRL Aerodynamics Range was designed to evaluate the Eley Tenex, RWS R-50, and Ultra Match rounds. In addition, custom-loaded rounds, whose bullets were similar in shape to the Eley and RWS bullets, but loaded to above and below standard velocities, were provided by Mr. Chernicky. The purpose of the firings at non-standard velocities was to determine a possible optimum muzzle velocity for minimizing the sensitivity of the bullet to crosswind.

Two Olympic-grade match rifles – an Anschutz Prone Rifle and a Remington 40-X Rifle – were obtained on loan by Ms. Beasley, and delivered to the BRL in early September, 1989. A total of 21 data rounds were fired through the BRL Aerodynamics Range between September 7th and September 15th, all of which produced useful data. This report presents the aeroballistic data collected in the BRL Aerodynamics Range, and the results of six-degrees-of-freedom trajectory calculations for the effects of wind on the caliber .22 Long Rifle trajectories.

II. Test Procedure and Material

The four ammunition types tested are illustrated in the photograph of Figure 1. The Eley Type Nose is a custom bullet, similar in shape to the Eley Tenex, which was tested at nominal muzzle velocities of 1200 feet/second (fps), 1075 fps and 975 fps. Ultra Match rounds were loaded to produce the same nominal muzzle velocities as the Eley Type Nose rounds.

Figure 2 is a photograph of the Anschutz Prone Rifle used for part of the program; Figure 3 is a photograph of the Remington 40-X Rifle used for the remainder of the test firings. Two rifles were used in an attempt to determine if different guns produced any significant differences in the observed aeroballistic characteristics of the Eley Tenex ammunition.

Figure 4 is a photograph of the BRL Aerodynamics Range (circa 1958), and Figure 5 illustrates the local and master coordinate systems for the range. The Aerodynamics Range is an enclosed, climate-controlled range, instrumented with spark-photography stations to record the motion of the projectile over 90 metres of its trajectory. The measurement accuracy of the range is to within 0.3mm in distance, 1 microsecond in time, and about 0.1 degree in pitch and yaw angles. The high-precision measurements permit determination of the drag to within less than 1 percent error, and the gyroscopic stability to within 2 percent error.

Physical measurements were taken on a sample of three projectiles of each type. The average physical properties of the four projectile types are listed in Table 1. Contour measurements were also obtained using a Mann optical comparator, and Figures 6 and 7 show the average dimensions of the Eley Tenex and the Ultra Match bullets, respectively. The RWS R-50 and Eley Type Nose contours were very similar to the Eley Tenex, and are not illustrated.

Both test rifles had uniform rifling twist rates of one turn in 16 inches of travel. Yaw induction was necessary on several of the test rounds, since the very small yaw obtained naturally from the match rifles and ammunition did not allow determination of the lift, overturning moment, and gyroscopic stability. A half-muzzle yaw inducer was utilized for several shots, in an attempt to induce more than the normal one degree yaw level, but the muzzle pressure of caliber .22 Long Rifle ammunition proved too low for this technique to work. However, adequate yaw levels of 3 to 5 degrees were obtained by firing the projectile through a tipping card, a thin cardboard placed at a 45 degree angle to the trajectory, about 5 metres ahead of the muzzle.

The round-by-round aerodynamic data obtained for the four caliber .22 match bullets are listed in Tables 2 through 5. Flight motion parameters for the four bullets are listed in Tables 6 through 9.

III. Aeroballistic Results

1. Flowfield Observations

An interesting and useful by-product of spark-photography range testing is the high quality flowfield visualization provided by the spark shadowgraphs. Figures 8 through 20 show the flowfields around the four bullet types tested, at low supersonic, transonic, and subsonic speeds. Figures 8 through 11 illustrate the small-yaw flowfields around the RWS R-50 and Eley Tenex bullets; the shock waves observed in these shadowgraphs are typical of bluff bodies flying at transonic speeds. The shock waves become weaker with decreasing Mach number, corresponding to the observed decrease in the drag coefficients.

Figures 12, 13 and 16 show the detached bow shock wave standing ahead of the nose, for the Eley Type Nose and Ultra Match bullets at low supersonic speeds. Figure 13, at Mach 1.01, shows that the bow shock has moved well ahead of the projectile, and is rapidly becoming a normal shock, as predicted by transonic flow theory. Figure 17, at Mach 0.99,

shows the disappearance of the bow shock wave, but it also shows locally supersonic flow over most of the projectile surface. Figures 11 and 20 show weak shocks persisting down to Mach 0.85, and confirm that the caliber .22 match bullets are still in the transonic flow regime at this speed.

All the shadowgraphs shown in Figures 8 through 20 were selected from range stations at which the angle of attack was less than 1/2 degree. Additional comments on the flowfield detail will be made at appropriate points in the discussion of the individual aerodynamic coefficients.

2. Aerodynamic Characteristics

The free-flight spark range data were fitted to solutions of the linearized equations of motion. The resulting flight motion parameters were used to infer linearized aerodynamic coefficients, using the methods of Reference 2. Preliminary analysis of the aerodynamic data showed distinct variations of several coefficients with yaw level. In Reference 3, Murphy has shown that aerodynamic coefficients derived from the linearized data reduction can be used to infer the coefficients in a nonlinear force and moment expansion, if sufficient data are available. For the caliber .22 Long Rifle match bullets, sufficient data were obtained to permit determination of some nonlinear coefficients. A more detailed analysis of nonlinear effects is presented in the subtopics of this section, which discuss individual aerodynamic coefficients.

a. Drag Force Coefficient

The drag coefficient, C_D , is determined by fitting the time-distance measurements from the range flight. C_D is distinctly nonlinear with yaw level, and the value determined from an individual flight reflects both the zero-yaw drag coefficient, C_{D_0} , and the induced drag due to the average yaw level of the flight. The drag coefficient variation is expressed as an even power series in yaw amplitude:

$$C_D = C_{D_0} + C_{D_{\delta^2}} \delta^2 + \dots \quad (1)$$

where C_{D_0} is the zero-yaw drag coefficient, $C_{D_{\delta^2}}$ is the quadratic yaw-drag coefficient, and δ^2 is the total angle of attack squared.

Analysis of the drag coefficient data for the caliber .22 match bullets gave the following average values of $C_{D_{\delta^2}}$ for the various bullet types:

Bullet Type	$C_{D_{\delta^2}}$
Eley Tenex/RWS R-50	5.1
Eley Type Nose	7.0
Ultra Match	9.6

The above values of the yaw-drag coefficient were used to correct the range values of C_D to zero-yaw conditions. Figures 21 through 23 show the variation of the zero-yaw drag coefficients with flight Mach number for the various match bullets.

Figure 21 is a plot of C_{D_0} versus Mach number for the Eley Tenex and RWS R-50 bullets. Statistical analysis of the drag coefficient data by means of Student's t-test showed no significant difference in C_{D_0} between Eley Tenex and RWS R-50 ammunition fired from the Anschutz rifle, or between the Anschutz and Remington 40-X rifles firing the same lot (Lot WI-682) of Eley Tenex ammunition. The solid curve of Figure 21 is drawn through the mean of all the data points, and the dashed portions indicate the drag coefficient trends at Mach numbers speeds above and below those tested. The round-to-round standard deviation in C_{D_0} for the Eley Tenex and RWS R-50 ammunition is 0.005, or about 2 percent.

Figure 22 illustrates the variation of C_{D_0} with Mach number for the custom-loaded Eley Type Nose projectile. For all flight Mach numbers below 0.97 (velocity below 1090 fps at standard atmospheric conditions), the Eley Type Nose bullet shows higher drag than the Eley Tenex and the R-50. Inspection of the shadowgraphs shown as Figures 8 and 14 indicates the reason for the observed difference. All three bullets had the nominal shape of Figure 6 when loaded into the rifle chamber. However, the Eley Tenex and R-50 bullets are softer alloys (Brinell Hardness Number 7.4 - 7.6) than the alloy used in the Eley Type Nose and Ultra Match bullets (Brinell Hardness Number 10). The acceleration imparted to the bullet on firing causes the ogive to set back, or slump, and for the softer Eley Tenex and R-50 bullets, the shoulder at the junction of the ogive and cylindrical center section is virtually swaged out. The harder Eley Type Nose bullet suffers less deformation on firing, and the in-flight shape is much closer to the as-loaded shape, with most of the shoulder left intact. The shock wave standing on the ogive just upstream of the shoulder in Figure 14 is the primary cause of the higher drag coefficient for the Eley Type Nose. Figures 11 and 15 show the same relative flowfield differences between the Eley Tenex and the Eley Type Nose designs at lower speeds. Over the Mach number range from 0.975 down to 0.80, the Eley Type Nose bullet averages 13 percent higher drag than the Eley Tenex and RWS R-50 bullets.

The variation of the zero-yaw drag coefficient with Mach number for the Ultra Match bullet is shown in Figure 23. The current Ultra Match design also shows higher zero-yaw drag than the Eley Tenex and RWS R-50 bullets. The shoulder at the junction of the ogive and cylinder is relatively small for the Ultra Match design, hence the higher drag does not appear to be related to the shoulder. Figure 7 shows that the ogive of the current Ultra Match bullet is nearly 1/4 caliber shorter than that of the Eley Tenex, and comparison of the flowfields past the Eley Tenex bullet (Figure 9) and the Ultra Match bullet (Figure 18), at nearly the same Mach number, indicate that the higher pressure on the short Ultra Match ogive causes a stronger recompression shock to form at the junction of the ogive and the cylindrical center section. Figures 10 and 19 illustrate the persistence of this flowfield difference at lower speeds, and explain the observation that the current Ultra Match bullet averages 8 percent higher drag than the Eley Tenex and RWS R-50 bullets, over the Mach number range from 0.975 down to 0.80.

b. Overturning Moment Coefficient

The overturning moment coefficient, $C_{M\alpha}$, is proportional to the product of the two characteristic epicyclic frequencies of the pitching and yawing motion. Thus the coefficient is well determined only if both epicyclic frequencies are accurately measured. The yaw level of caliber .22 match bullets fired from match rifles is generally under one degree, which does not permit good determination of the epicyclic frequencies. Only the rounds fired through a tipping card to induce yaw provided satisfactory determination of the transverse aerodynamic force and moment coefficients. The RWS R-50 ammunition was not fired through tipping cards, thus only the drag coefficient was determined for the R-50 bullet design.

No significant variation of the overturning moment coefficient with yaw level could be found for any of the caliber .22 match bullets tested. The range values of $C_{M\alpha}$ are plotted against Mach number in Figures 24 through 26 for the Eley Tenex, Eley Type Nose, and Ultra Match bullets, respectively.

The trends of the three curves are similar, with peak values of $C_{M\alpha}$ occurring near Mach 0.96, which is typical of the overturning moment coefficient for short, bluff projectiles with flat bases.⁴ The Eley Type Nose design averages ten percent higher $C_{M\alpha}$ than the Eley Tenex bullet over the Mach number range 0.975 down to 0.80; the average overturning moment coefficient for the Ultra Match design over the same speed interval is nearly identical to that of the Eley Tenex bullet.

c. Gyroscopic Stability

The gyroscopic stability factor of a projectile is defined⁶ as:

$$S_g = \frac{P^2}{4M} \quad (2)$$

where:

$$P = \left(\frac{I_x}{I_y} \right) \left(\frac{p d}{V} \right)$$

$$M = \left(\frac{\rho S d^3}{2 I_y} \right) C_{M\alpha}$$

The remaining symbols are defined in the List of Symbols in this report.

Figure 27 illustrates the variation of launch gyroscopic stability factor with launch Mach number for the three caliber .22 match bullets. The Eley Tenex and Ultra Match bullets, fired at a nominal launch Mach number of 0.97 (1090 fps) from the standard rifling

twist rate of 16 inches/turn, at standard ICAO sea-level atmospheric conditions, have a launch gyroscopic stability factor of 1.5, which is sufficient to provide stable flight under all weather conditions, including cold (high density) air.

The launch gyroscopic stability factor of the Eley Type Nose bullet fired under the same conditions is 1.25, which is too low for satisfactory use in cold weather. However, the Eley Type Nose bullet is an experimental test design, and will not be loaded for use in competition; therefore, its low gyroscopic stability factor is irrelevant.

d. Lift Force Coefficient

The lift force coefficient, $C_{L\alpha}$, is plotted against Mach number in Figure 28 for the three match bullets tested. No significant variation of $C_{L\alpha}$ with yaw level could be found for any of the match bullet designs.

The Ultra Match design shows approximately fifteen percent higher average lift than do the Eley Tenex and Eley Type Nose bullets. The lift force coefficient is determined from the center-of-mass swerving motion, and swerve is less well determined in spark-photography ranges than is the pitching and yawing motion. This fact is reflected in the larger round-to-round data scatter observed in Figure 28, compared with the overturning moment coefficient data plotted in Figures 24 through 26.

e. Magnus Moment Coefficient and Pitch Damping Moment Coefficient

The Magnus moment coefficient, $C_{M_{p\alpha}}$, and the pitch damping moment coefficient, $(C_{M_q} + C_{M_{\dot{\alpha}}})$, are discussed together, since if either coefficient is nonlinear with yaw level, both coefficients exhibit nonlinear coupling in the data reduction process.³ Due to mutual interaction, the analysis of $C_{M_{p\alpha}}$ and $(C_{M_q} + C_{M_{\dot{\alpha}}})$ must be performed simultaneously, although the aerodynamic moments are not, in themselves, physically related.

If the dependence of the Magnus moment and the pitch damping moment are cubic in yaw level, the nonlinear variation of the two moment coefficients is of the general form:

$$C_{M_{p\alpha}} = C_{M_{p\alpha 0}} + \hat{C}_2 \delta^2 \quad (3)$$

$$(C_{M_q} + C_{M_{\dot{\alpha}}}) = (C_{M_q} + C_{M_{\dot{\alpha}}})_0 + d_2 \delta^2 \quad (4)$$

where $C_{M_{p\alpha 0}}$ and $(C_{M_q} + C_{M_{\dot{\alpha}}})_0$ are the zero-yaw values of Magnus and pitch damping moment coefficients, respectively, and \hat{C}_2 and d_2 are the associated cubic coefficients.

In Reference 3 it is shown that the non-linear coupling introduced through the least-squares data reduction process yields the following expressions for range values [R-subscript] of $C_{M_{p\alpha}}$ and $(C_{M_q} + C_{M_{\dot{\alpha}}})$:

$$[C_{M_{\rho\alpha}}]_R = C_{M_{\rho\alpha 0}} + \bar{C}_2 \delta e_{TT}^2 + d_2 \delta e_{TH}^2 \quad (5)$$

$$[(C_{M_q} + C_{M_{\dot{\alpha}}})]_R = (C_{M_q} + C_{M_{\dot{\alpha}}})_0 + \bar{C}_2 \delta e_{HH}^2 + d_2 \delta e_{HT}^2 \quad (6)$$

where the above effective squared yaws are defined as:

$$\delta e_{TT}^2 = K_F^2 + K_S^2 + \frac{(\phi'_F K_F^2 - \phi'_S K_S^2)}{(\phi'_F - \phi'_S)} \quad (7)$$

$$\delta e_{TH}^2 = \left(\frac{I_x}{I_y} \right) \left[\frac{(K_F^2 \phi'_F^2 - K_S^2 \phi'_S^2)}{(\phi'_F - \phi'_S)} \right] \quad (8)$$

$$\delta e_{HH}^2 = \left(\frac{I_y}{I_x} \right) \left[\frac{(\phi'_F + \phi'_S)(K_S^2 - K_F^2)}{(\phi'_F - \phi'_S)} \right] \quad (9)$$

$$\delta e_{HT}^2 = \frac{(\phi'_F K_S^2 - \phi'_S K_F^2)}{(\phi'_F - \phi'_S)} \quad (10)$$

The remaining symbols are defined in the List of Symbols in this report.

Preliminary analysis of the caliber .22 match bullet data showed significant nonlinearity in the range values of $C_{M_{\rho\alpha}}$ and $(C_{M_q} + C_{M_{\dot{\alpha}}})$ at angles of attack less than two degrees, with weaker nonlinear trends at larger yaw levels. The data rounds were separated into Mach number groups, by bullet type, and an analysis was performed to determine the cubic coefficients at both small and large yaw levels. No statistically significant values of the cubic pitch damping moment coefficient, d_2 , could be found.

The data were then analyzed assuming a cubic Magnus moment and linear pitch damping moment. Further analysis revealed no significant variation of either coefficient with bullet type, and all match bullet types were combined for final analysis.

Figures 29 and 30 illustrate the results obtained for the caliber .22 match bullets. Figure 29 shows a bi-cubic behavior of the Magnus moment coefficient with yaw level. For angles of attack under two degrees ($\delta_e^2 < .0015$), the Magnus moment coefficient increases rapidly with increasing yaw level, growing from -0.8 at zero yaw to essentially zero at two degrees yaw. For larger angles of attack, the bi-cubic coefficient appears to depend on the Mach number region. At transonic speeds the Magnus moment coefficient is approximately zero for angles of attack greater than two degrees. At subsonic speeds (Mach number < 0.80), the coefficient begins to decrease slowly for yaw levels exceeding two degrees.

Figure 30 shows the zero-yaw pitch damping moment coefficient, corrected for the cubic Magnus effect. No significant variation with either Mach number or bullet type is observed. The average value of $(C_{M_q} + C_{M_{\dot{\alpha}}})_0$ does not differ statistically from zero, indicating that the caliber .22 match bullets experience virtually no pitch damping moment at transonic and subsonic speeds.

IV. Flight Dynamic Characteristics

The BRL six-degrees-of-freedom (6-DOF) flight simulation program⁵ was used to investigate the flight dynamic characteristics of the Eley Tenex ammunition. The average observed muzzle velocity of 1090 fps was used, and standard ICAO sea-level atmospheric conditions were assumed. The standard rifling twist rate of 16 inches/turn and the physical and aerodynamic characteristics of the Eley Tenex bullet were input to the 6-DOF computer program. An initial yaw rate of 11 radians/second was used, which produced a first maximum yaw of one degree.

Six-degrees-of-freedom trajectories were run to a range of 100 metres, and the results showed that the fast epicyclic yaw arm damps to less than 0.2 degree at 25 metres range. However, the cubic Magnus moment coefficient (Figure 29) causes the slow arm to be unstable at yaw levels under 1.8 degrees, but stable at larger yaw levels. The result is a slow-arm limit cycle yaw of approximately 1.8 degrees. The slow arm reaches the limit cycle value at about 50 metres range, and adds approximately 2 percent to the drag.

Neither the retained velocity nor the accuracy are significantly degraded by the small slow-arm limit cycle yaw. The Eley Tenex ammunition exhibits generally good flight dynamic characteristics over the ranges for which it is used in competitive shooting. Although no flight dynamic measurements were made for the RWS R-50 ammunition, its observed similarity to the Eley Tenex in physical characteristics, drag coefficient, and flowfield properties suggests very similar flight dynamic characteristics for the two bullets.

The Ultra Match bullet tested at BRL was an early prototype design, and the current design is significantly different in several respects. Flight dynamic results for the original Ultra Match design are no longer relevant, and are not presented.

V. Wind Sensitivity Results

A study of the sensitivity of Eley Tenex ammunition to wind was done using the BRL 6-DOF flight simulation program. The six-degrees-of-freedom method completely accounts for the effect of wind on the trajectory, unlike the point-mass trajectory models commonly used. However, for small-yaw flight, the results of 6-DOF wind calculations agree quite closely with the classical point-mass models and the linearized ballistic theory, as will be demonstrated presently.

The 6-DOF wind study investigated the effect of three wind velocities and twelve wind directions for each velocity, for the Eley Tenex ammunition at a range of 50 metres. The wind directions are on a clock-based system, with the rifleman at the clock center and the target at twelve o'clock. A nine o'clock wind is blowing from left to right across the line of fire; a twelve o'clock wind is blowing from the target toward the firing line.

Figures 31 through 33 illustrate the 6-DOF results, with the standard 50 metre Olympic target drawn to scale, for wind velocities of 10 miles/hour (mph), 20 mph and 30 mph, respectively. The solid black data points represent the impact of bullets in the wind,

if the rifle is properly zeroed and the rifleman makes no wind corrections. The number adjacent to each impact point is the clock direction from which the wind is blowing.

All three figures exhibit the well-known 10 o'clock/4 o'clock slant, although for the Eley Tenex ammunition at 50 metres range, a 9:30/3:30 slant would be more precise. The 10/4 slant of groups has often been observed by bench-rest shooters when firing on windy days. Many explanations of this effect have been advanced in the popular literature; most of them are based on the principle of Magnus force.

If Magnus force were the cause of slanted groups in the wind, the direction would be reversed, i.e., an 8 o'clock/2 o'clock slant would result from firing a rifle with right-hand twist of rifling. In addition, modern spark-photography range firings have shown that the Magnus force acting on small-arms projectiles is too small to have any significant effect on the trajectory.

The 10/4 slant of groups in the wind from a right-hand twist of rifling is due to aerodynamic jump, which is an effective change in the vertical angle of departure of the trajectory, caused by the initial yaw due to the crosswind. A useful equation for calculating the aerodynamic jump will be given later in this section.

Figures 31 through 33 show that the wind response of Eley Tenex ammunition is essentially-linear in wind speed up to 30 mph; a 20 mph wind deflects the bullet twice as much as does a 10 mph wind. The present study indicates that the Eley Tenex ammunition is slightly more sensitive to wind than some previously published wind tables indicate, but the difference is of little practical importance.

Figure 31 shows that even a 10 mph crosswind (2-4 o'clock, or 8-10 o'clock) will cause the rifleman to lose one point on the scoring ring unless a vertical correction is made in addition to the usual horizontal windage correction. In a 20 mph crosswind, two points will be lost due to the vertical aerodynamic jump, even if the horizontal correction is properly made. The ratio of vertical to horizontal correction for the Eley Tenex ammunition at 50 metres range is approximately 1:4. If the rifleman needs to move the sight to the left to correct for a wind between 7 o'clock and 11 o'clock, 1 click of elevation should be added for each 4 clicks of left windage applied. If the sight needs to be moved to the right, 1 click of elevation should be subtracted for each 4 clicks of right windage.

The classical crosswind deflection formula, based on a point-mass trajectory assumption, is well known to most riflemen:

$$D_H = W \left(T - \frac{R}{V_0} \right) \quad (11)$$

where:

- D_H = horizontal deflection due to crosswind
- W = crosswind velocity
- T = time of flight to range R
- R = range to target
- V_0 = muzzle velocity

The aerodynamic jump due to crosswind acts in the vertical plane, and modifies the angle of departure of the trajectory. A modern discussion of aerodynamic jump is given by Murphy in Reference 6. The vertical deflection due to crosswind can be calculated by means of the following formula:

$$D_V = - \left(\frac{I_x}{m d^2} \right) \left(\frac{C_{L\alpha}}{C_{M\alpha}} \right) \left(\frac{2 \pi}{n} \right) \left(\frac{W}{V_0} \right) R \quad (12)$$

where:

D_V = vertical deflection due to crosswind

I_x = projectile axial moment of inertia

m = projectile mass

d = projectile reference diameter

$C_{L\alpha}$ = lift force coefficient

$C_{M\alpha}$ = overturning moment coefficient

n = rifling twist rate (calibers/turn)

Note that in Equation (12), n is considered positive for right hand twist of rifling, and negative for left-hand twist. A crosswind blowing from left to right is considered positive; a negative crosswind blows from right to left. On the target, a high impact is considered positive, as is an impact to the right.

For the Eley Tenex ammunition at 50 metres range, Equations (11) and (12) were used to calculate the bullet response to crosswind, and the results are illustrated in Figure 34. The agreement between the results of Figure 34 and those of Figure 31 is excellent, and indicates that six-degrees-of-freedom calculations are not necessary to accurately predict the effects of low-level winds on flat-fire trajectories. If the physical characteristics and the spark-photography range data are available to determine the necessary inputs for use in Equations (11) and (12), the calculation of wind sensitivity for small-arms projectiles can be done with sufficient accuracy for all practical purposes, using relatively simple ballistic methods.

The final part of the BRL wind study examined the effect of different muzzle velocities on the wind sensitivity of Eley Tenex ammunition. Muzzle velocities ranging from 1100 fps down to 800 fps were tried, with a 10 mph crosswind. The results showed that a muzzle velocity of approximately 950 fps gives minimum wind sensitivity for the Eley Tenex bullet, at both the 50 metre and 100 metre ranges. The wind sensitivity at a muzzle velocity of 950 fps would be approximately 20 percent less than that experienced at the standard velocity of 1090 fps.

VI. Conclusions

1. Spark-photography range firings were conducted with Eley Tenex and RWS R-50 ammunition, fired from Olympic-grade competition rifles. The measurements made led to an accurate assessment of the effects of wind on the trajectory of caliber .22 Long Rifle match ammunition used in Olympic competition.
2. No significant difference in drag was observed between Eley Tenex and RWS R-50 ammunition fired from the Anschutz rifle. No significant difference in drag was observed between the Anschutz rifle and the Remington 40-X rifle, firing the same lot of Eley Tenex ammunition. These results suggest that the choice of rifle or brand of match ammunition used has an insignificant effect on the wind sensitivity of caliber .22 Long Rifle bullets used in Olympic competition.
3. The round-to-round standard deviation in drag for Olympic-grade caliber .22 match ammunition is about 2 percent. The effect of 2 percent drag standard deviation on wind sensitivity is negligible at ranges of 50 and 100 metres.
4. The launch gyroscopic stability factor of caliber .22 match bullets, fired from rifles with a standard rifling twist rate of 16 inches/turn and at standard ICAO sea-level atmospheric conditions, is 1.5, which is sufficient to provide stable flight under all weather conditions, including cold (high density) air.
5. The nonlinear Magnus moment acting on caliber .22 match bullets at transonic and subsonic speeds causes a slow-arm limit cycle yaw of approximately 1.8 degrees. The slow arm grows to the limit cycle value at about 50 metres range, and the limit cycle persists out to 100 metres range. The limit cycle yaw adds approximately 2 percent to the zero-yaw drag, but has an insignificant effect on accuracy, retained velocity and wind sensitivity.
6. The effect of wind on the trajectory of caliber .22 match ammunition at 50 metres range is to cause bullet impacts distributed along a 9:37/3:30 slant line. The left/right deflection is accurately predicted by the classical wind drift formula, and the vertical deflection is accurately predicted by the ballistic formula for aerodynamic jump. The rifleman needs to make one click adjustment in elevation for every four clicks made on windage.
7. A muzzle velocity of approximately 950 fps would minimize the wind sensitivity of Eley Tenex and RWS R-50 bullets. The wind sensitivity at a muzzle velocity of 950 fps would be approximately 20 percent less than that experienced at the standard velocity of 1090 fps.

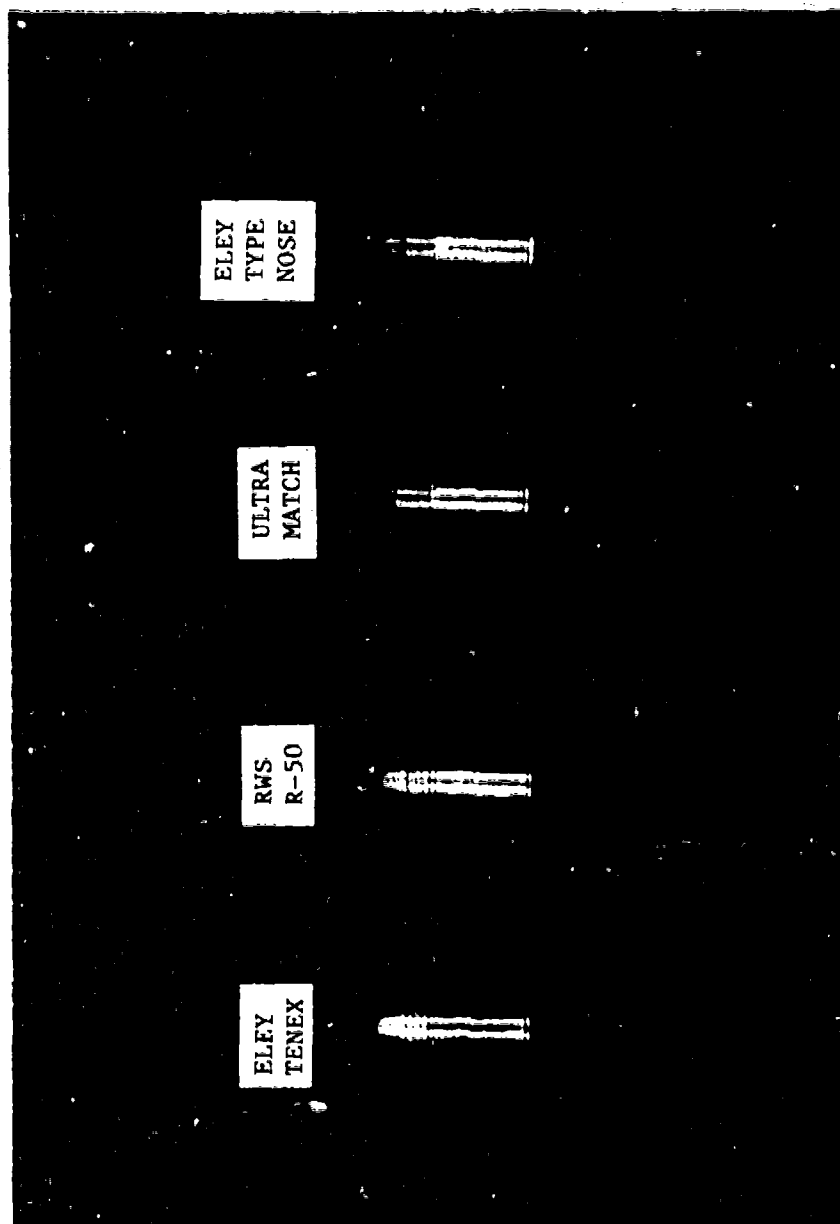


Figure 1. Photograph of caliber .22 long rifle match ammunition.

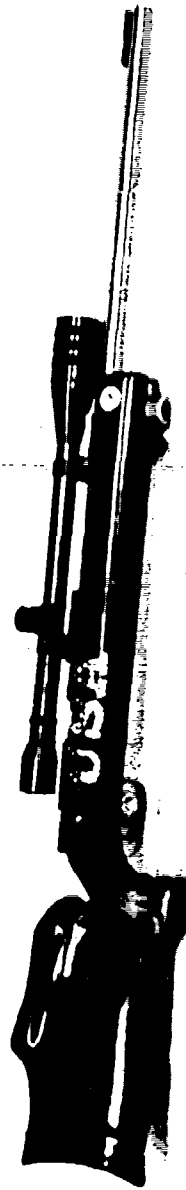


Figure 2. Photograph of the Anschutz prone rifle.

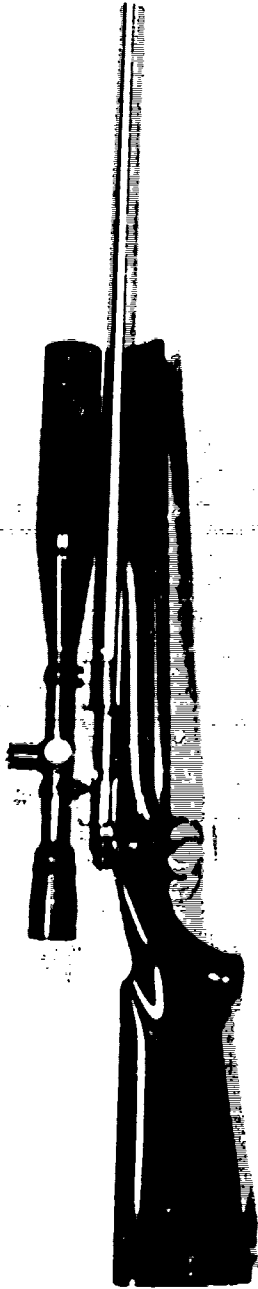


Figure 3. Photograph of the Remington 40-X rifle.



Figure 4. Photograph of the BRL free flight aerodynamics range.

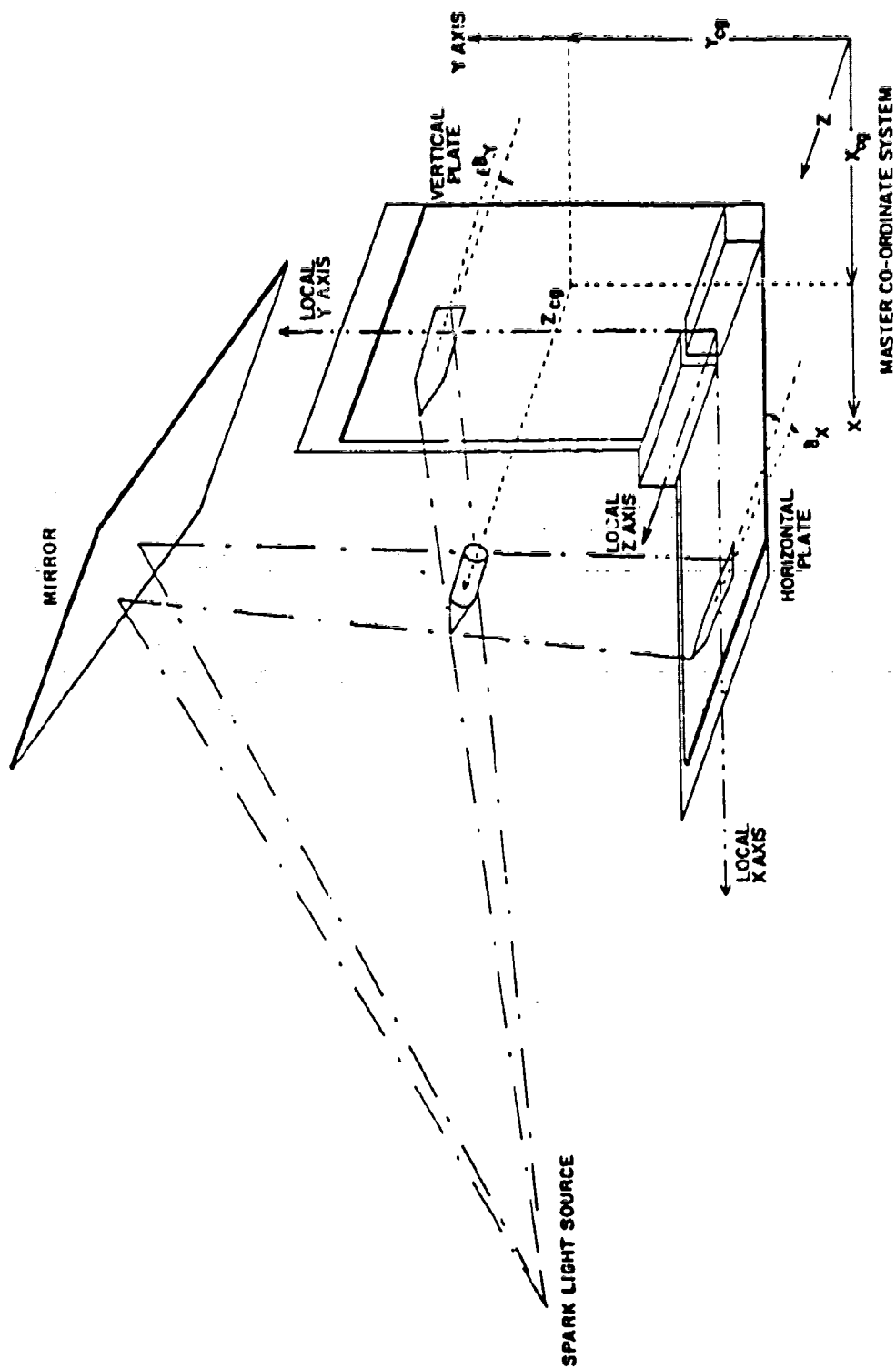
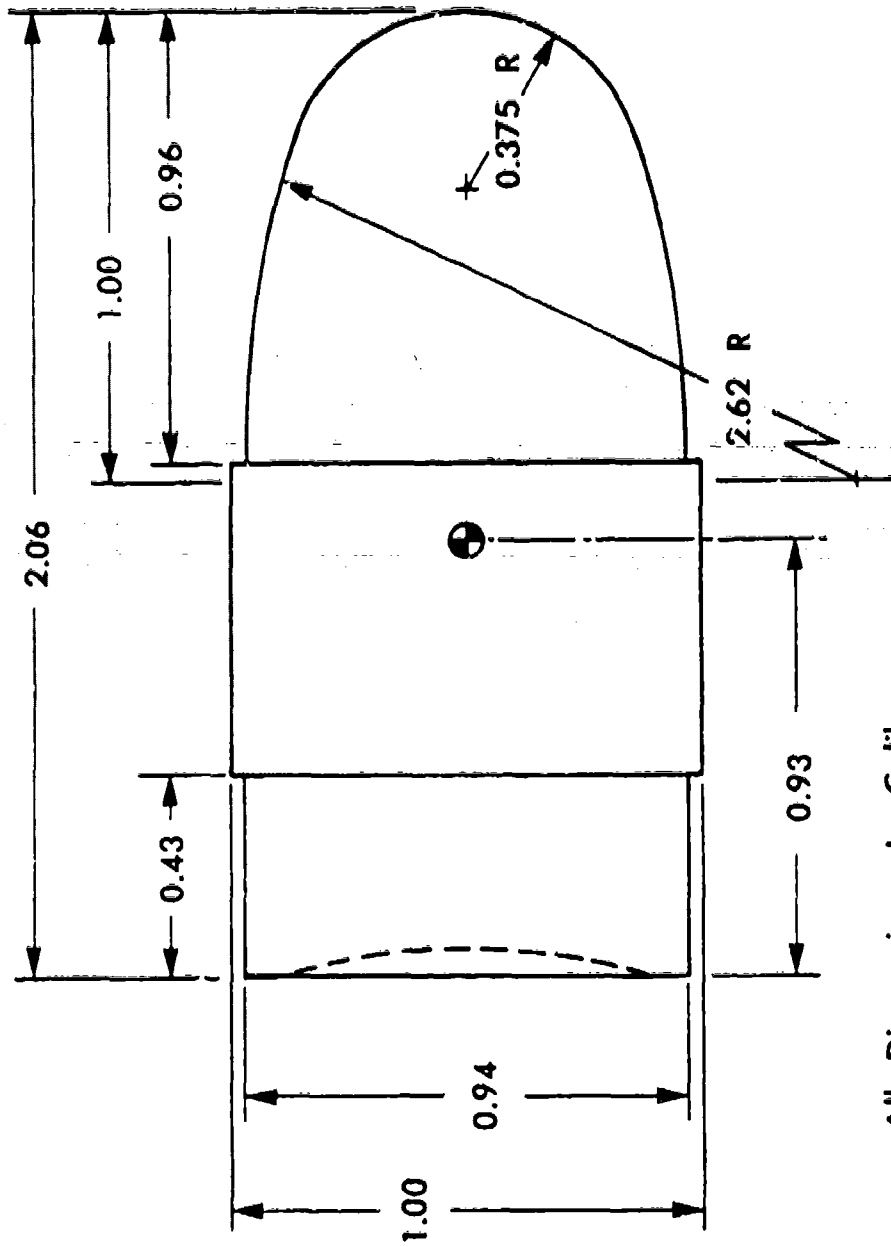


Figure 5. Coordinate system for the BRL aerodynamics range.

ELEY TENEX



All Dimensions in Calibers
(1 Caliber = 5.69 mm)

Figure 6. Sketch of the Eley Tenex bullet.

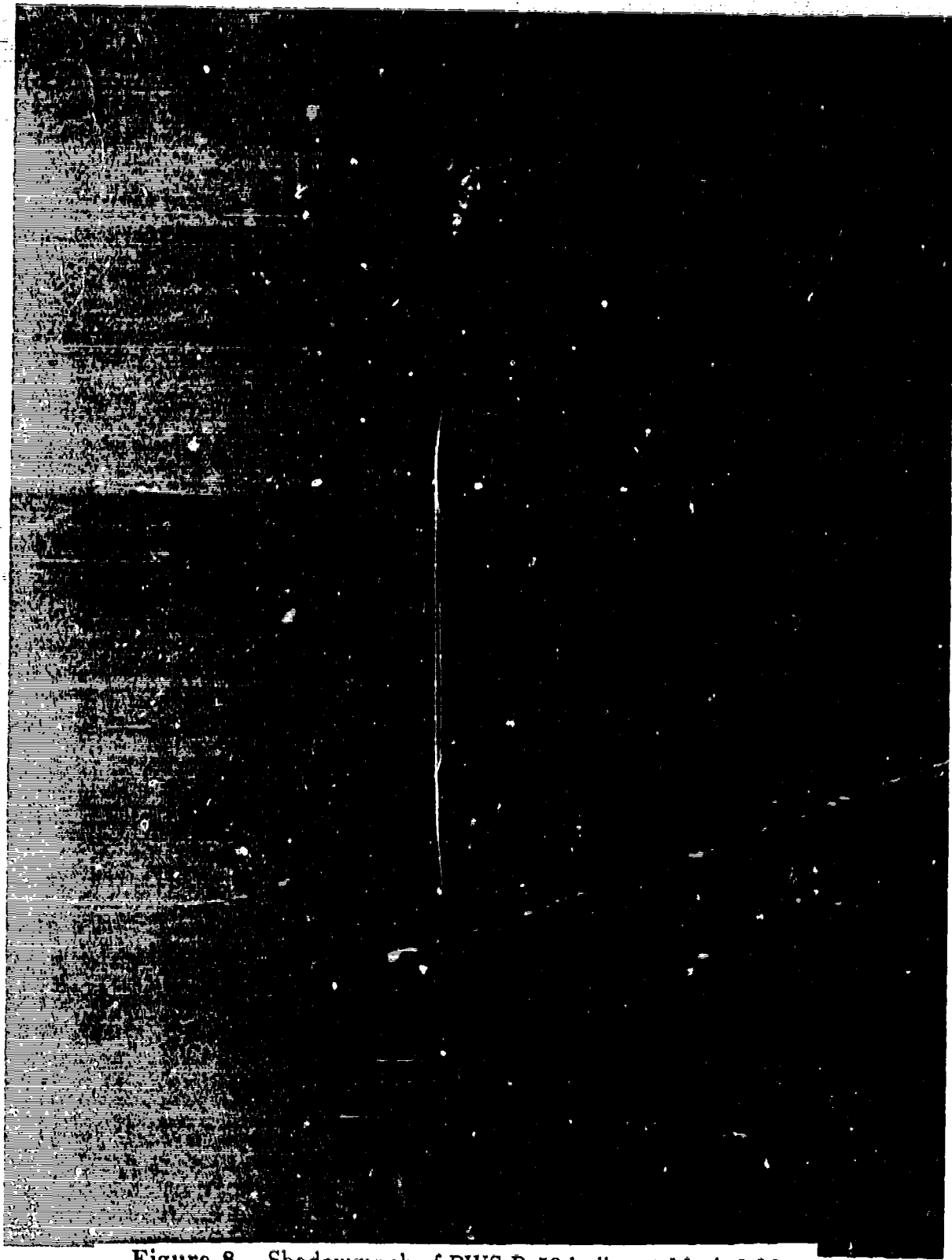


Figure 8. Shadowgraph of RWS R-50 bullet at Mach 0.96.

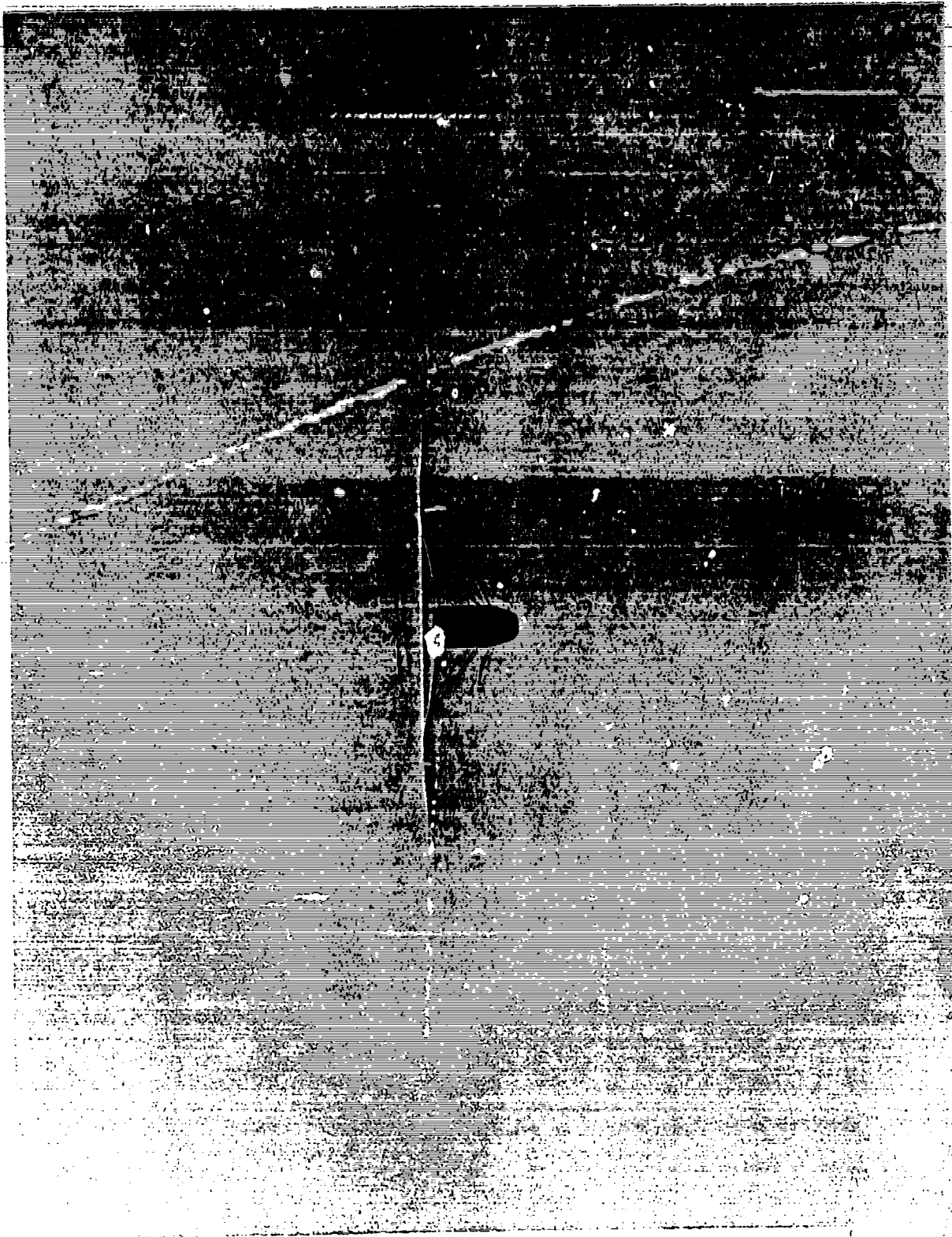


Figure 9. Shadowgraph of Eley Tenex bullet at Mach 0.95.

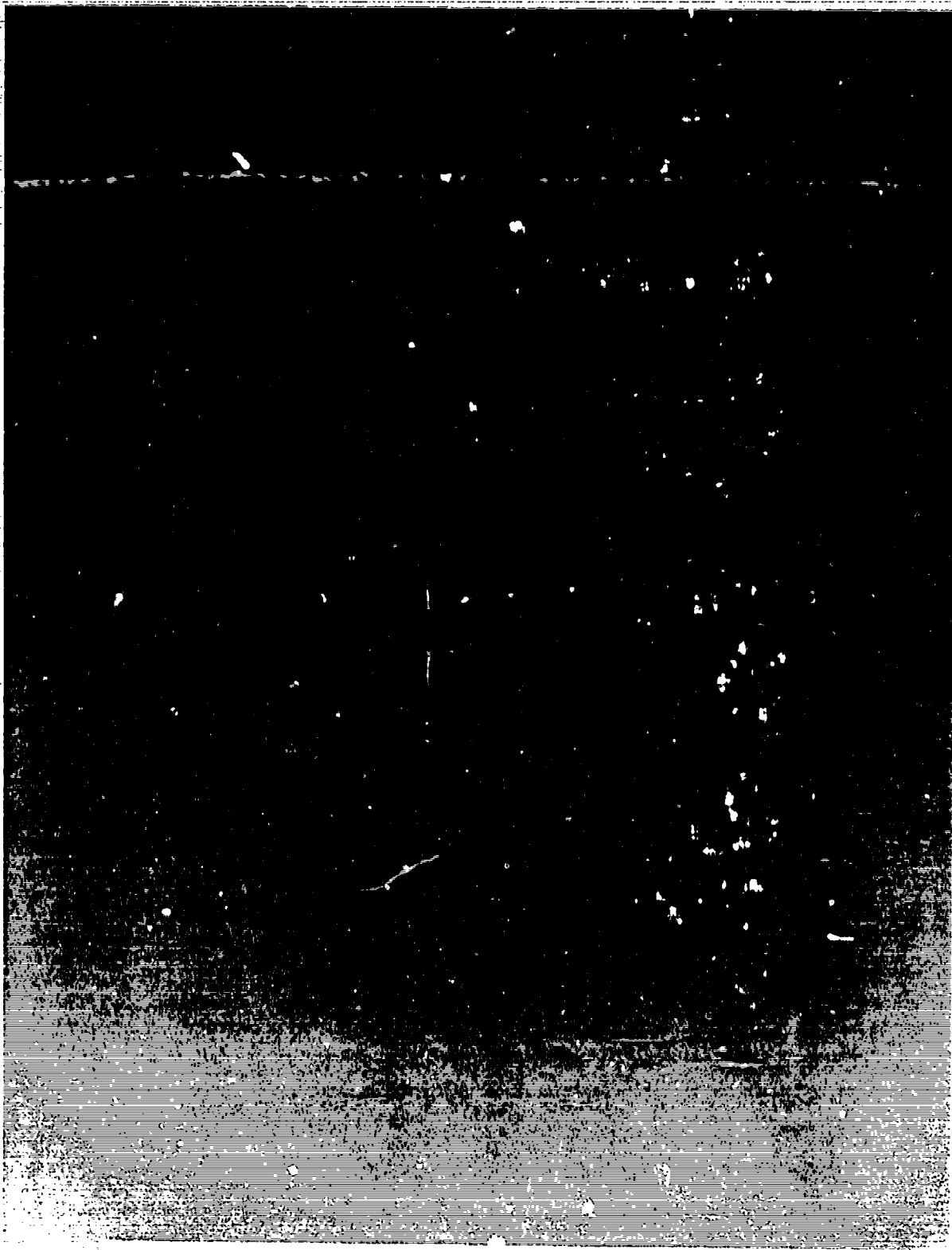


Figure 10. Shadowgraph of Eley Tenex bullet at Mach 0.90.

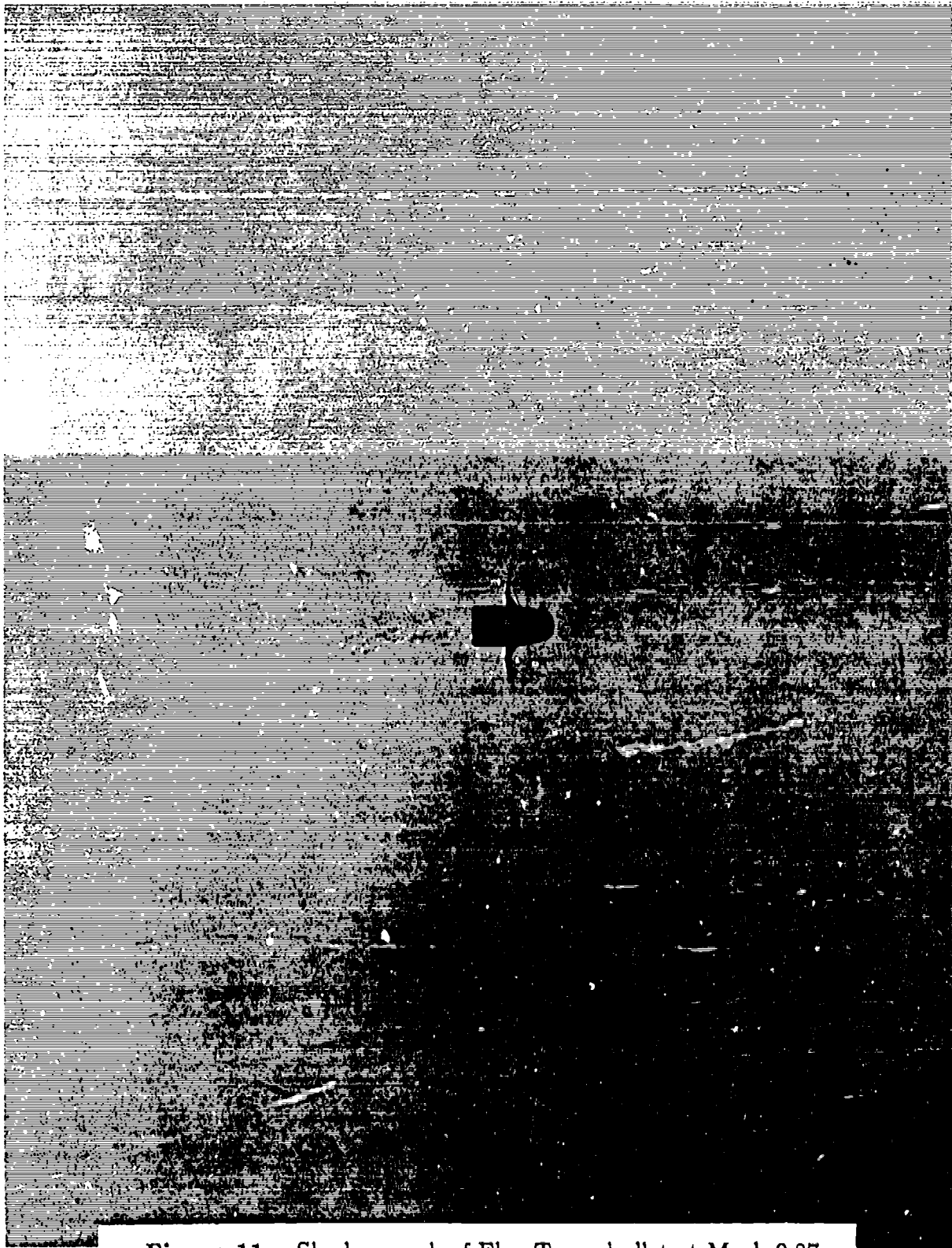


Figure 11. Shadowgraph of Eley Tenex bullet at Mach 0.87.

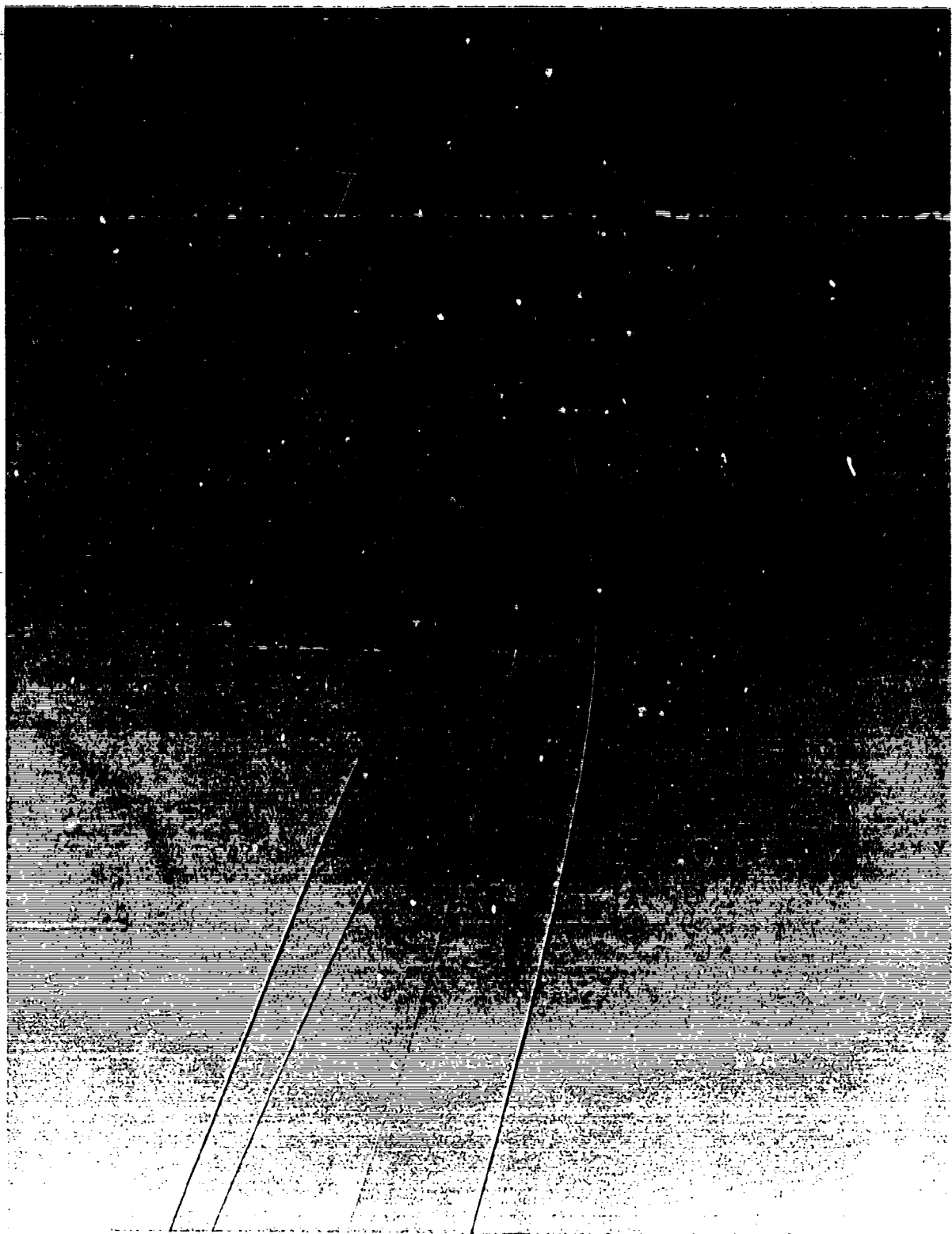


Figure 12. Shadowgraph of Eley type nose bullet at Mach 1.05.

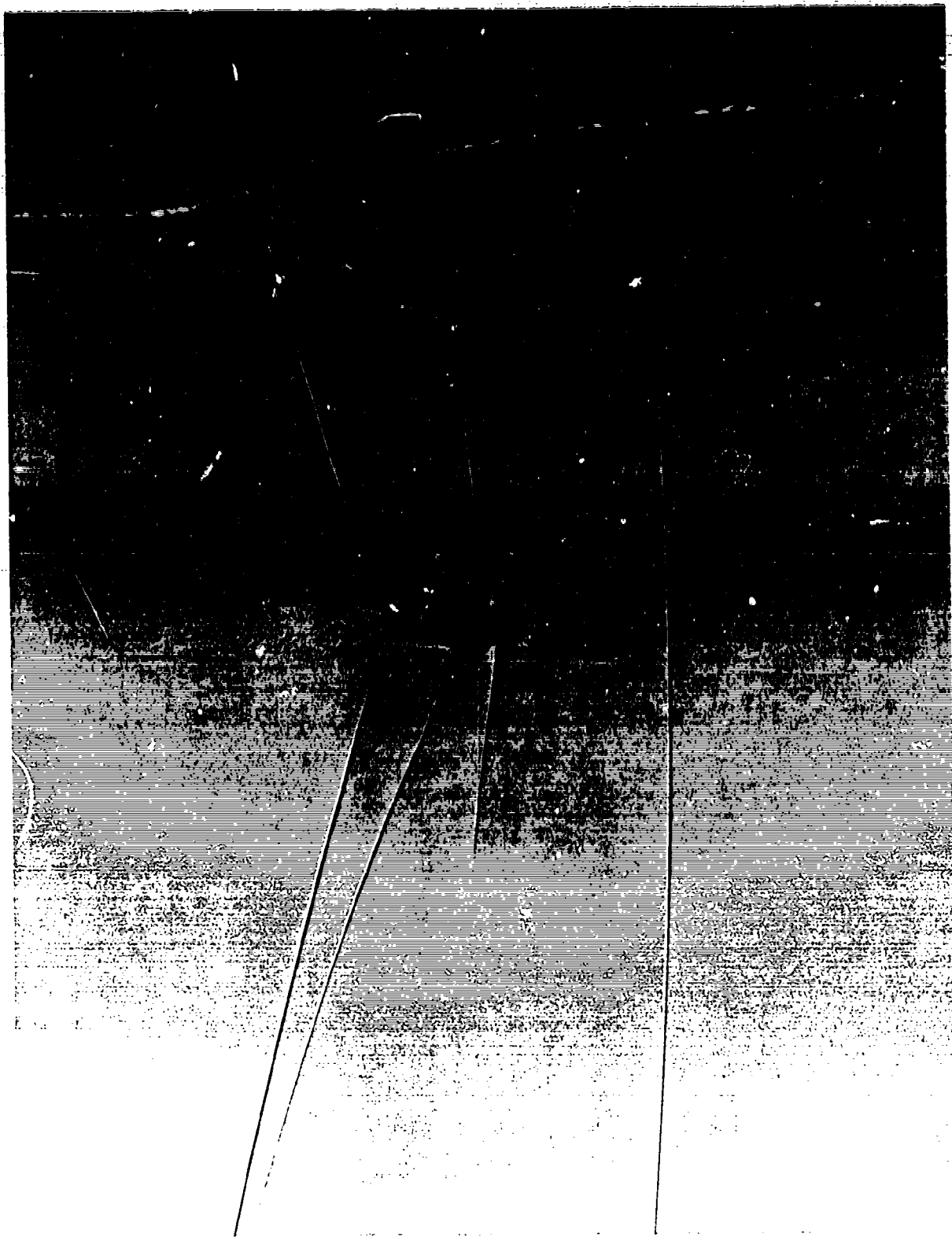


Figure 13. Shadowgraph of Eley type nose bullet at Mach 1.01.

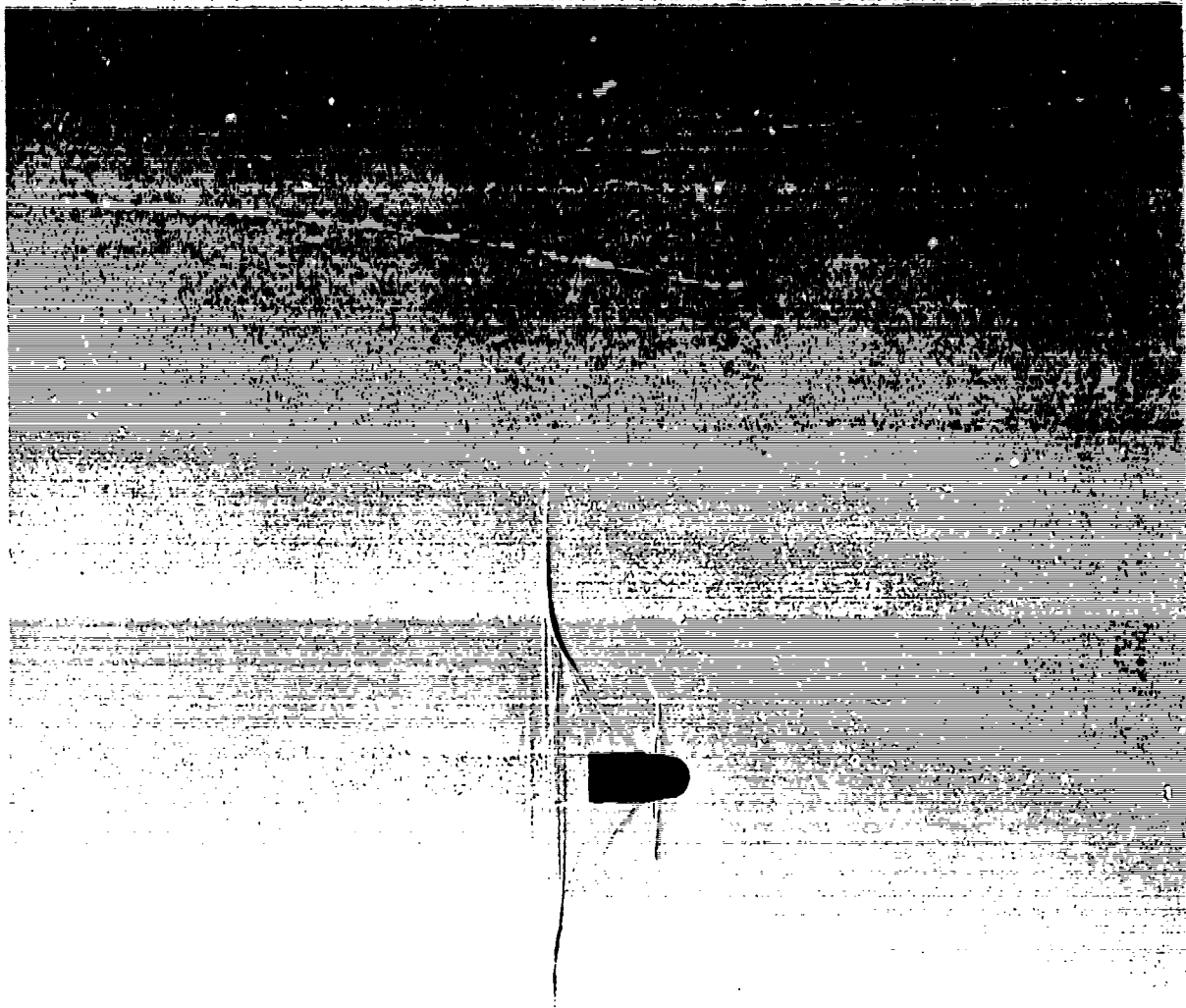


Figure 14. Shadowgraph of Eley type nose bullet at Mach 0.96.



Figure 15. Shadowgraph of Eley type nose bullet at Mach 0.89.



Figure 16. Shadowgraph of Ultra match bullet at Mach 1.05.

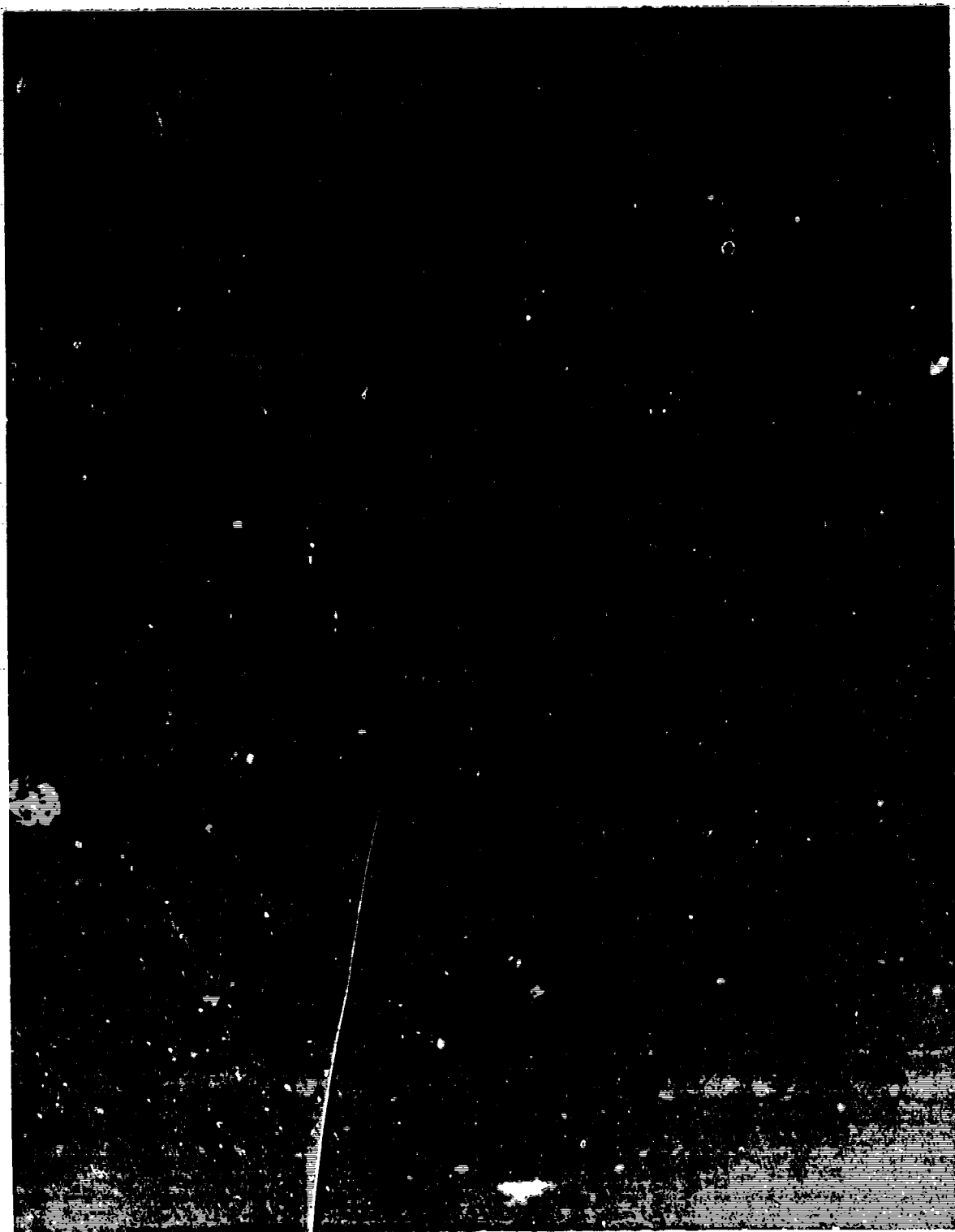


Figure 17. Shadowgraph of Ultra match bullet at Mach 0.99.

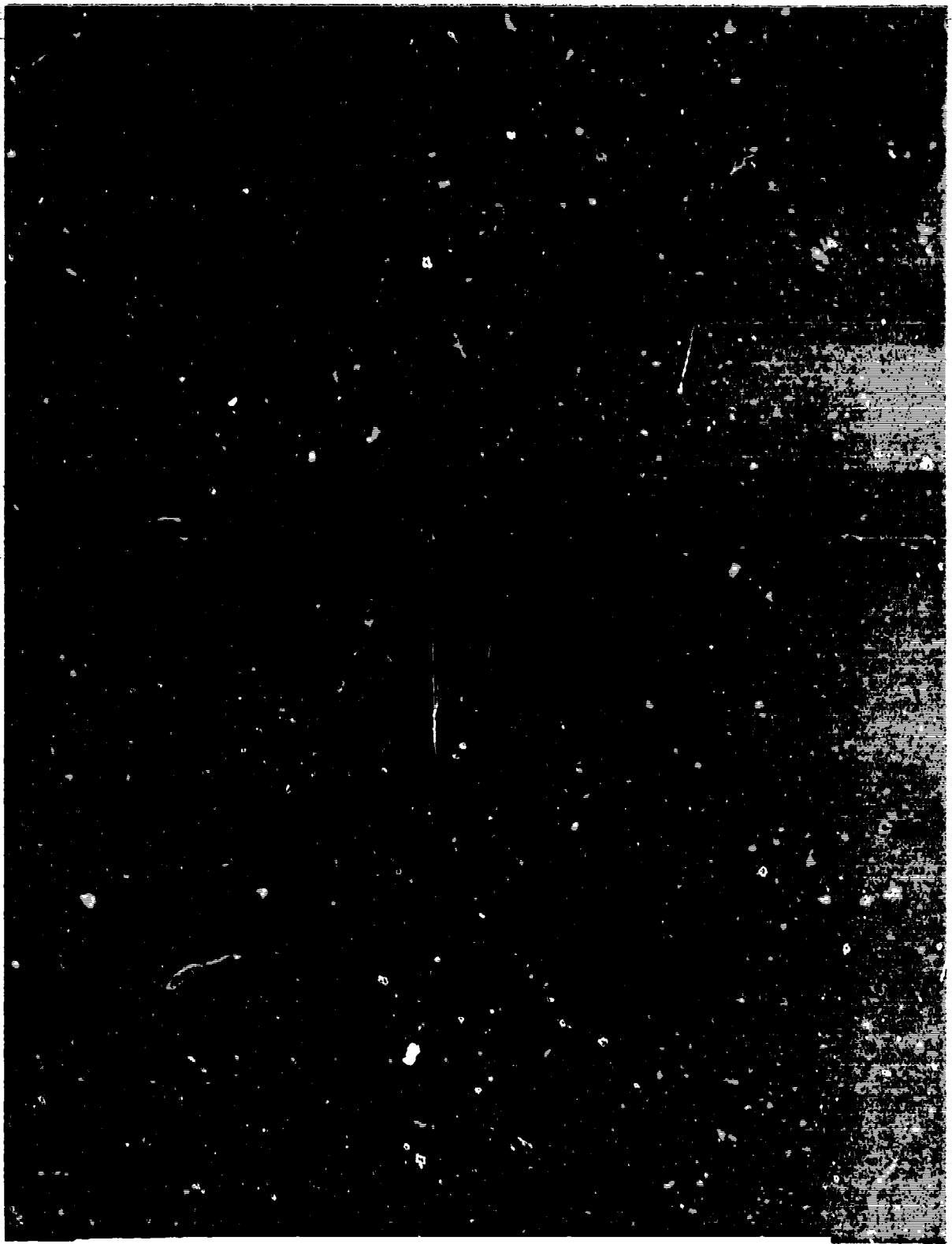


Figure 18. Shadowgraph of Ultra match bullet at Mach 0.94.

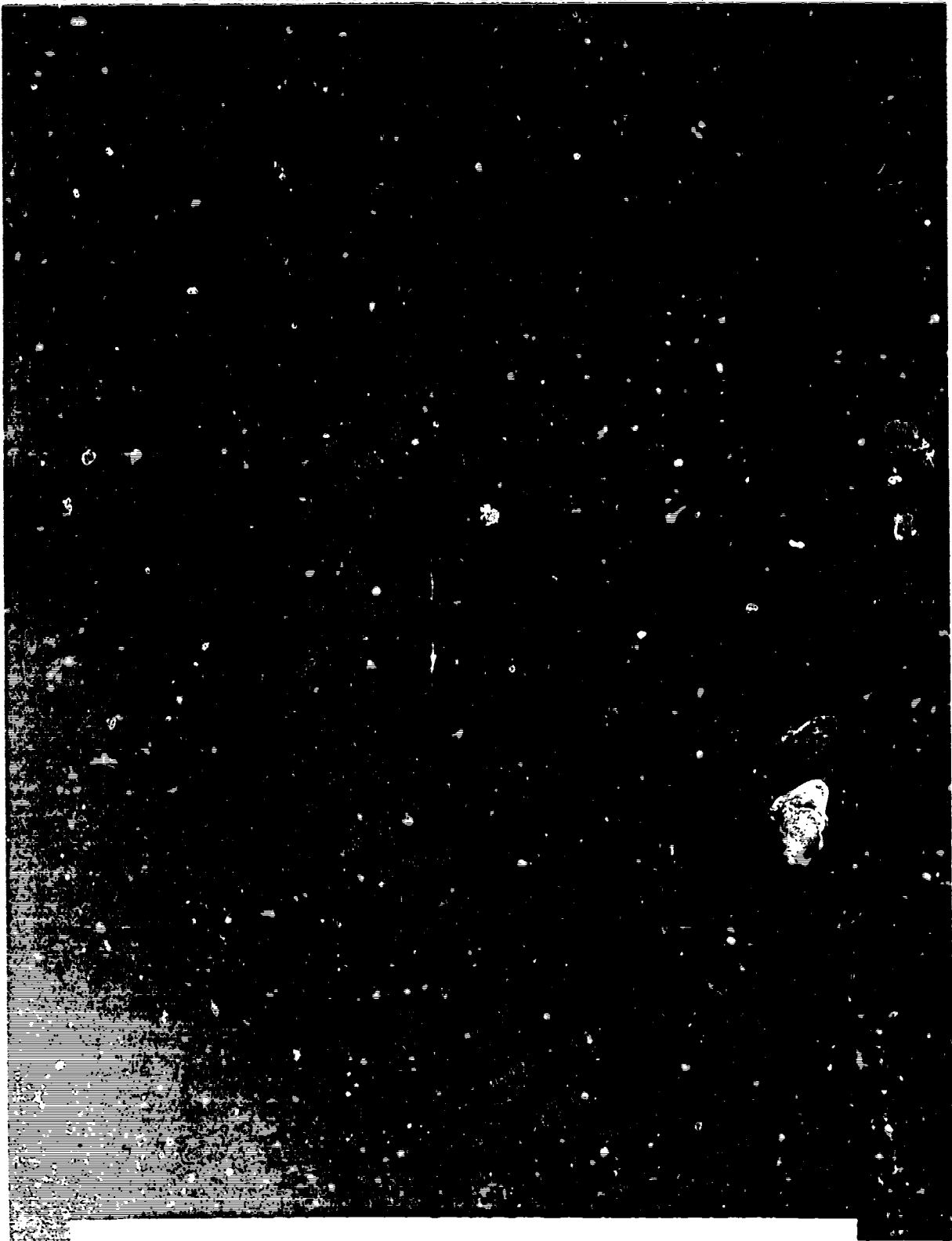


Figure 19. Shadowgraph of Ultra match bullet at Mach 0.91.



Figure 20. Shadowgraph of Ultra match bullet at Mach 0.85.

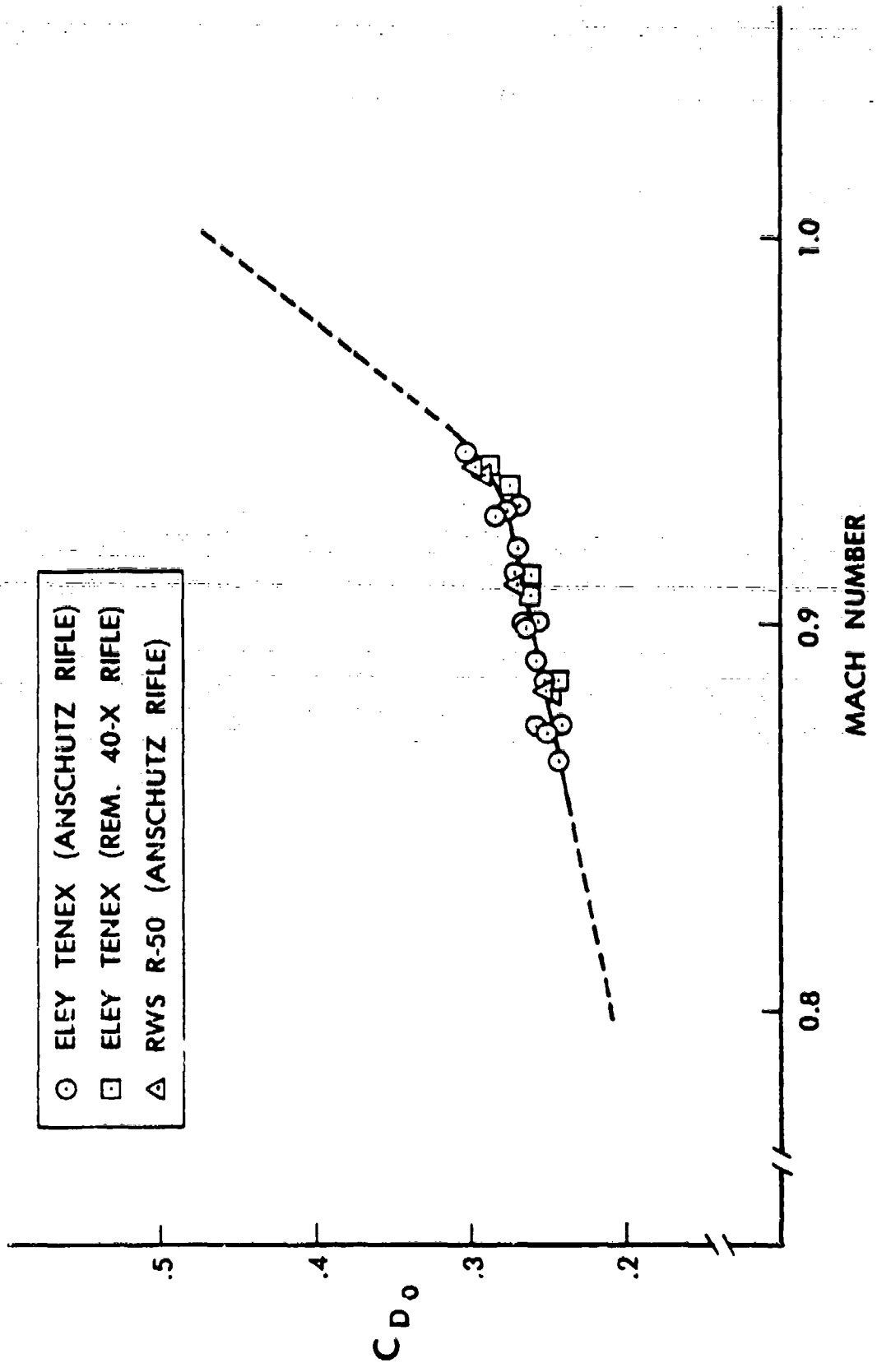


Figure 21. Zero-yaw drag force coefficient versus Mach number, Eley Tenex and RWS R-50 bullets.

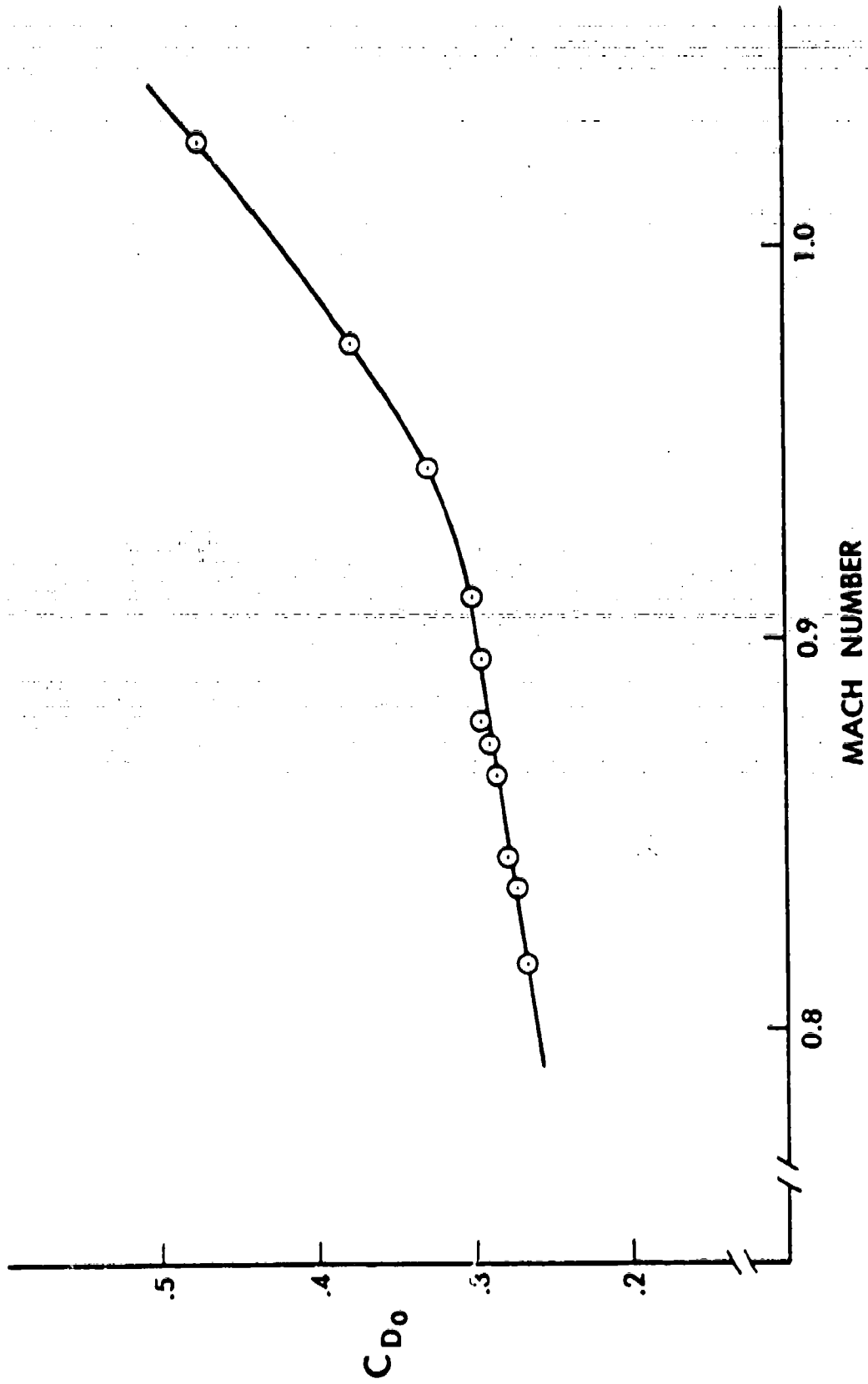


Figure 22. Zero-yaw drag force coefficient versus Mach number, Eley type nose bullet.

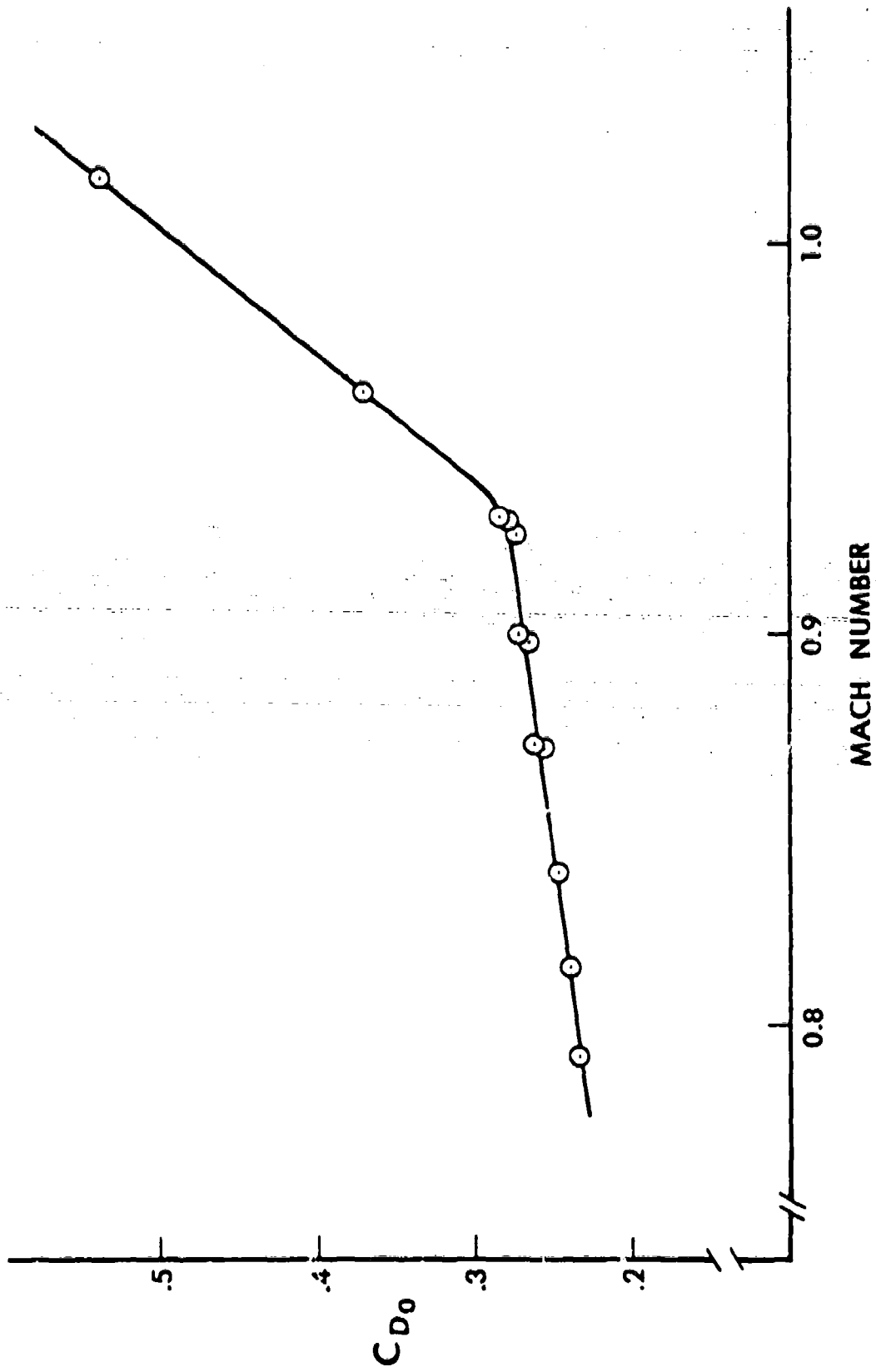


Figure 23. Zero-yaw drag force coefficient versus Mach number, Ultra match bullet.

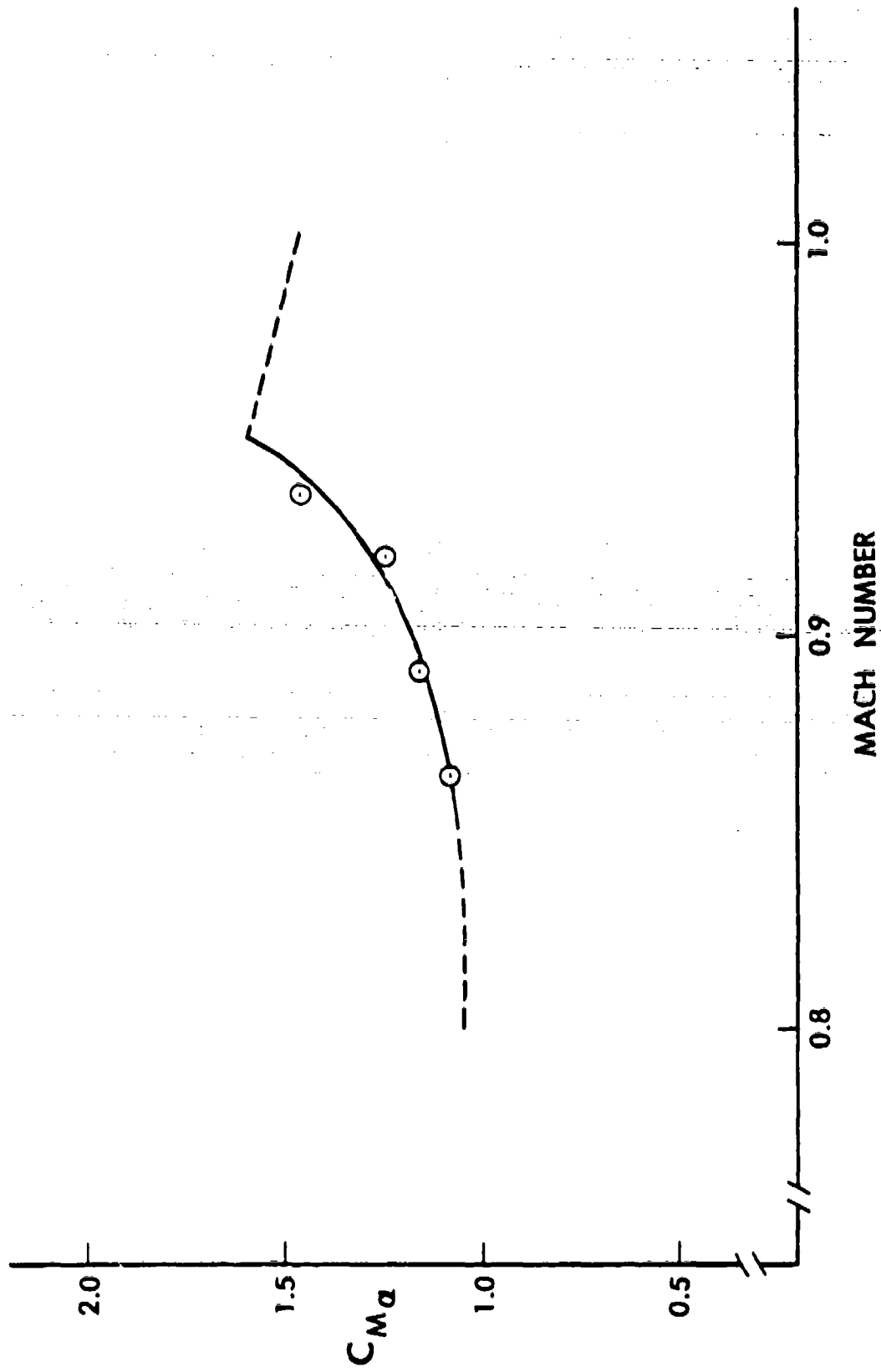


Figure 24. Overturning moment coefficient versus Mach number, Eley Tenex bullet.

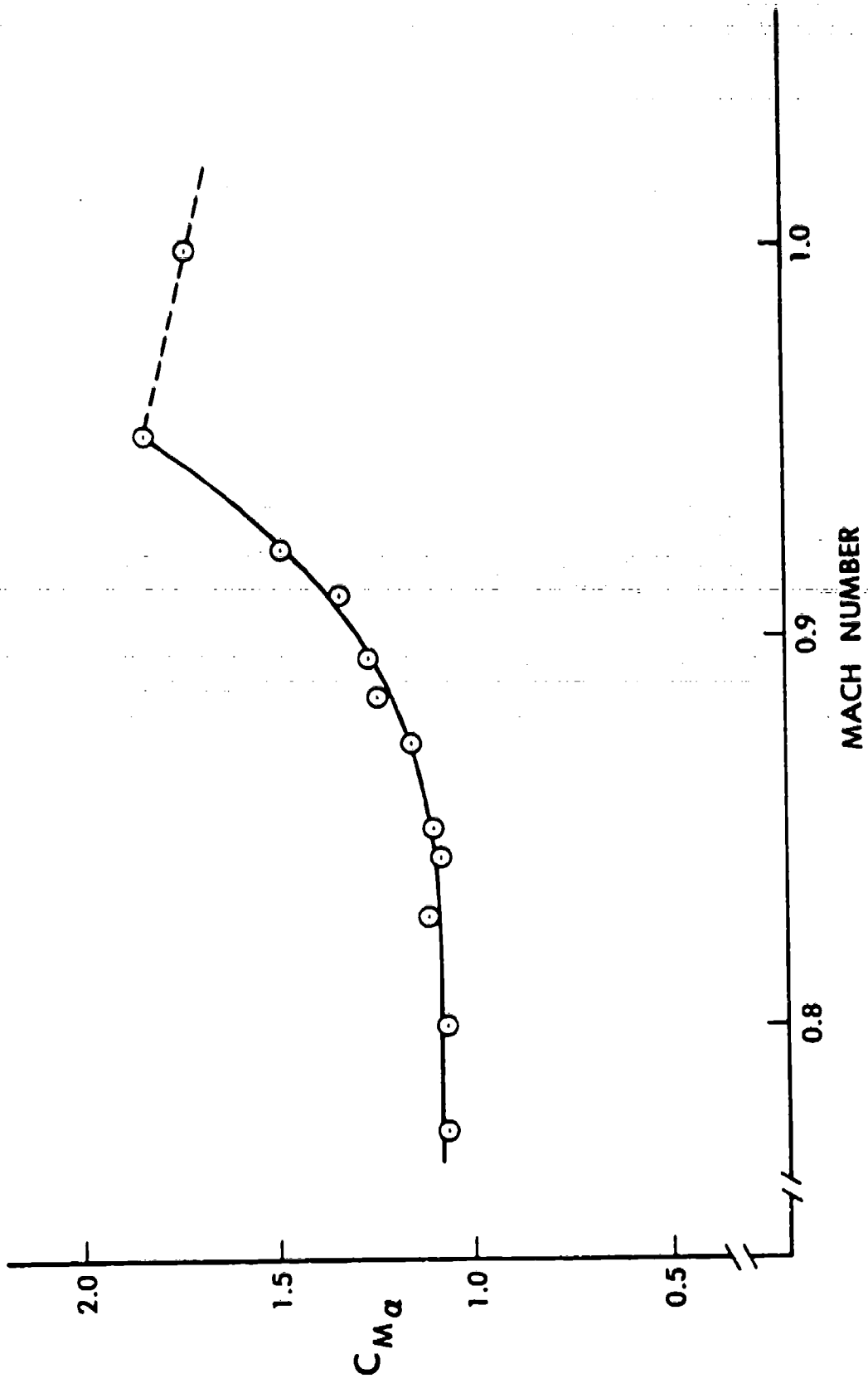


Figure 25. Overturning moment coefficient versus Mach number, Eley type nose bullet.

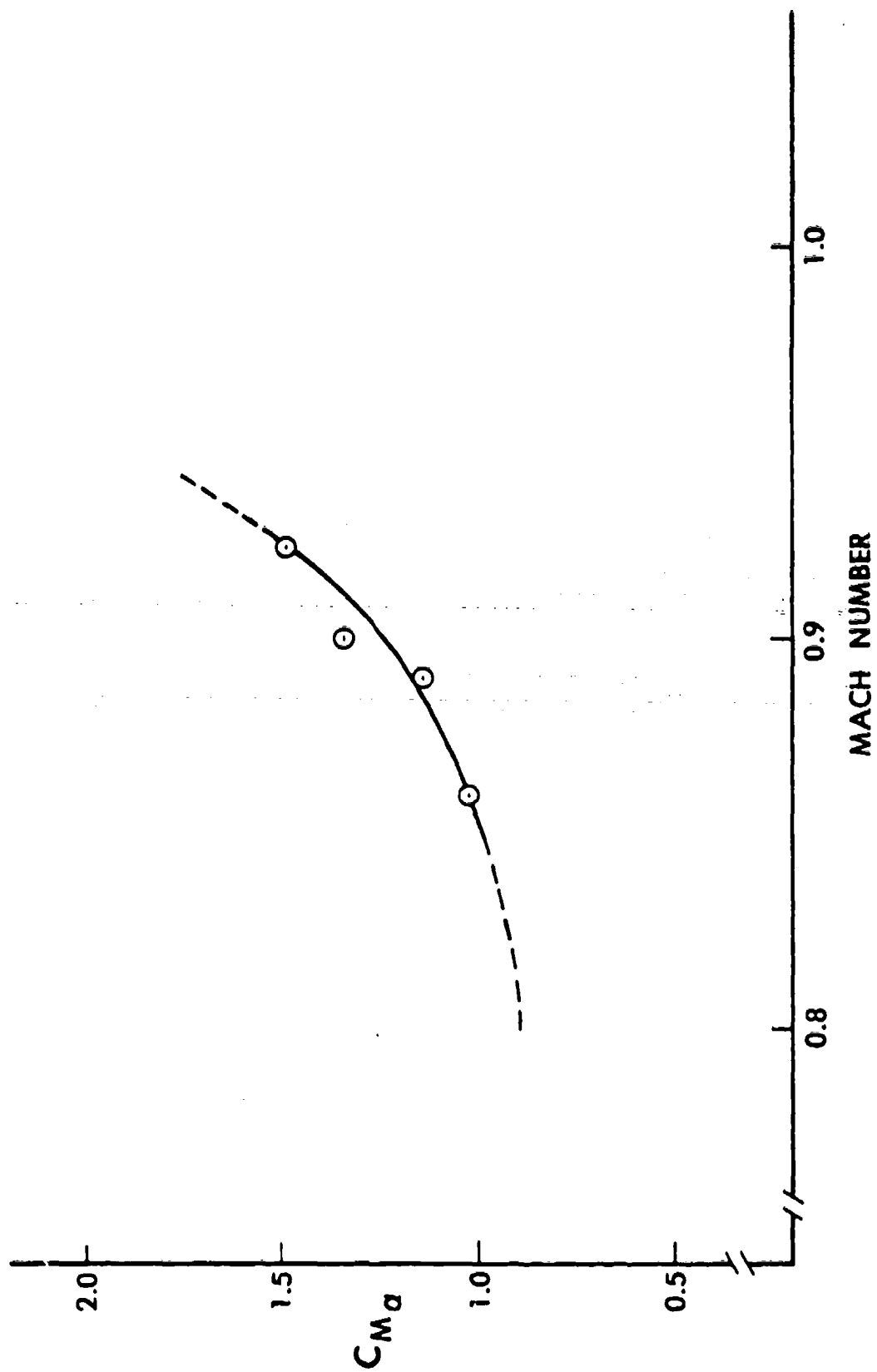


Figure 26. Overturning moment coefficient versus Mach number, Ultra match bullet.

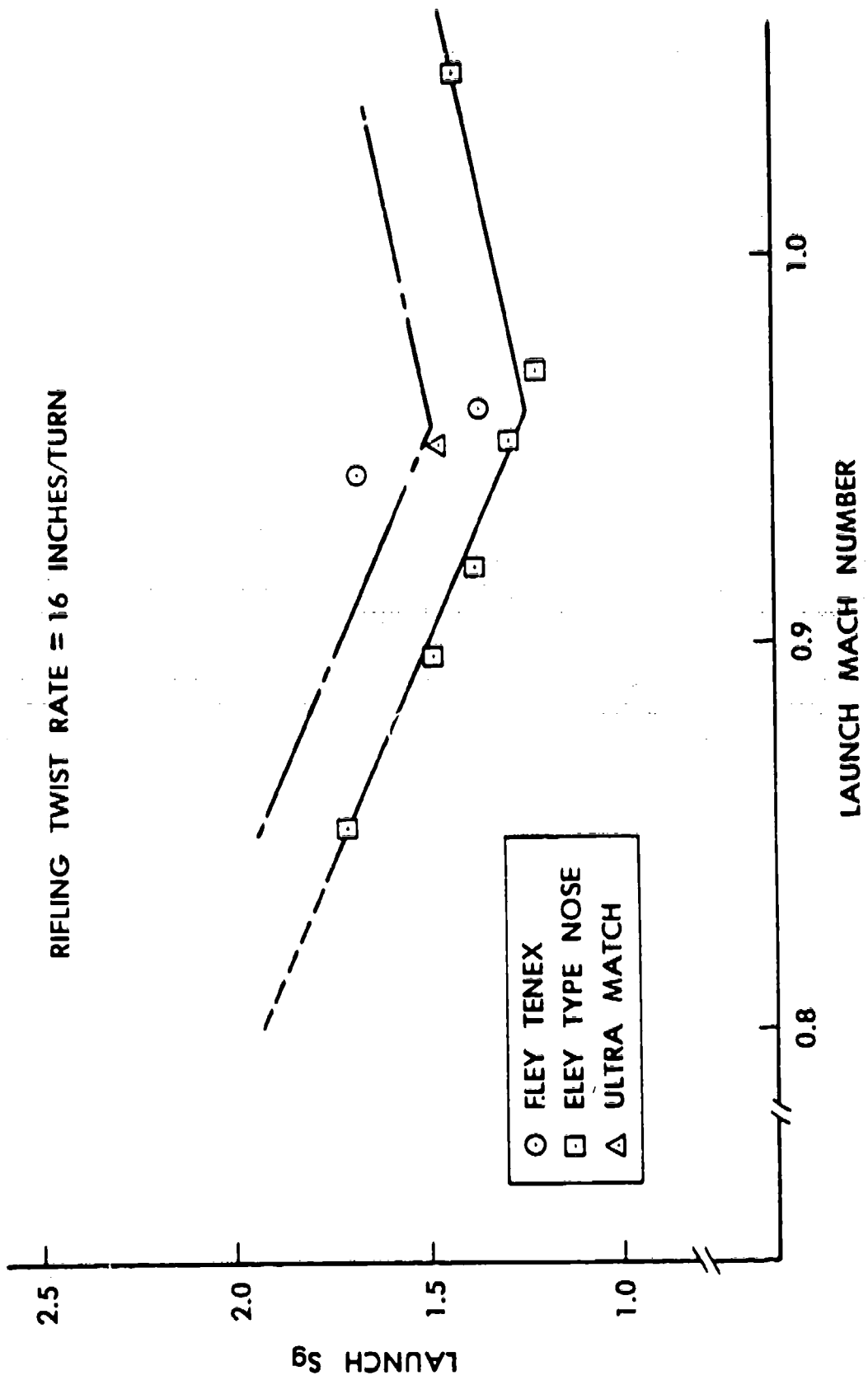


Figure 27. Launch gyroscopic stability factor versus launch Mach number.

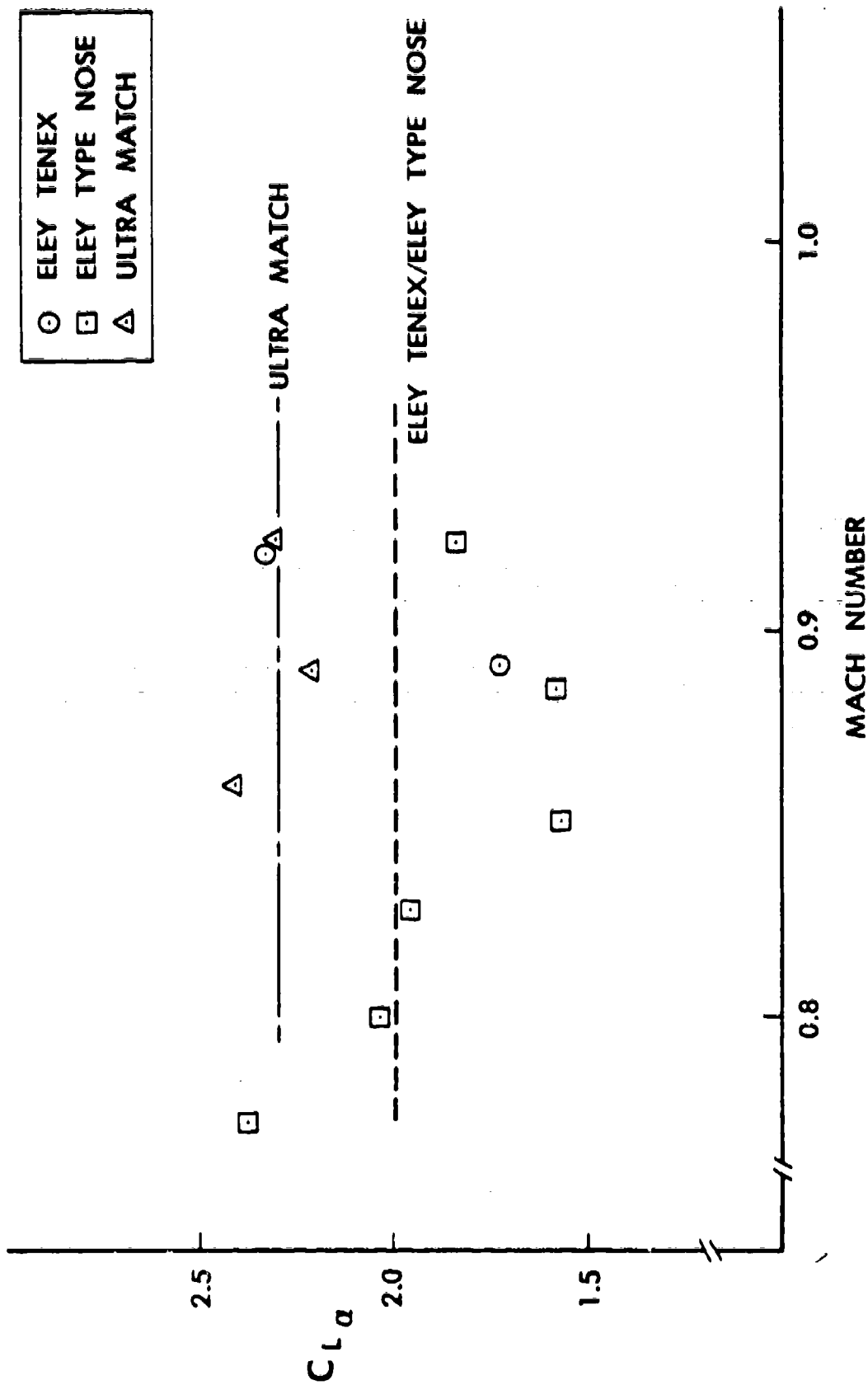


Figure 28. Lift force coefficient versus Mach number.

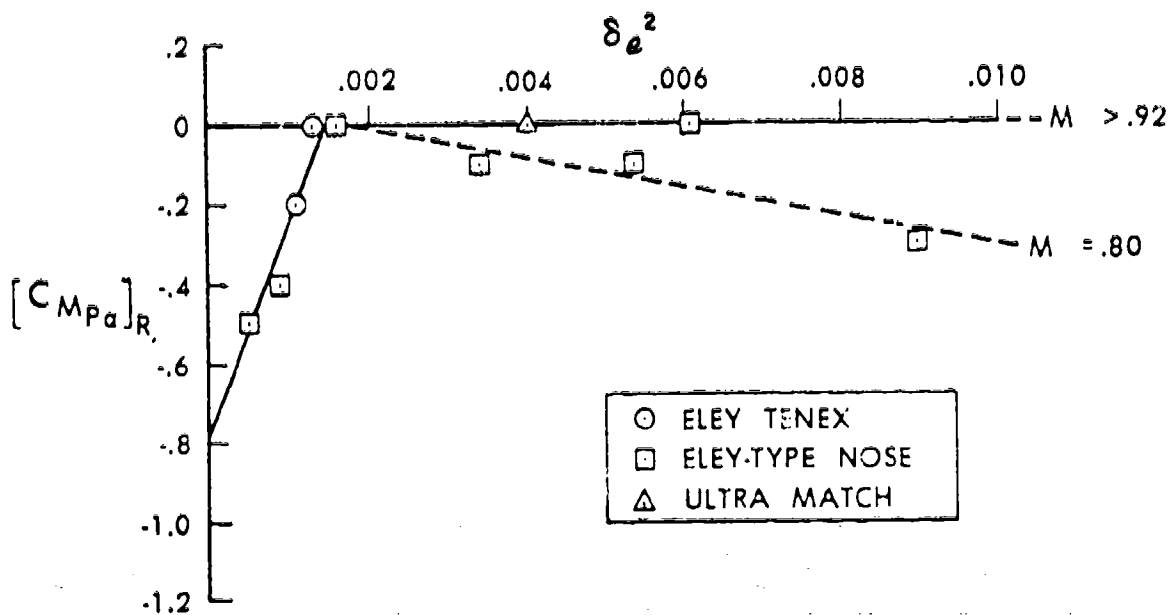


Figure 29. Magnus moment coefficient versus effective squared yaw.

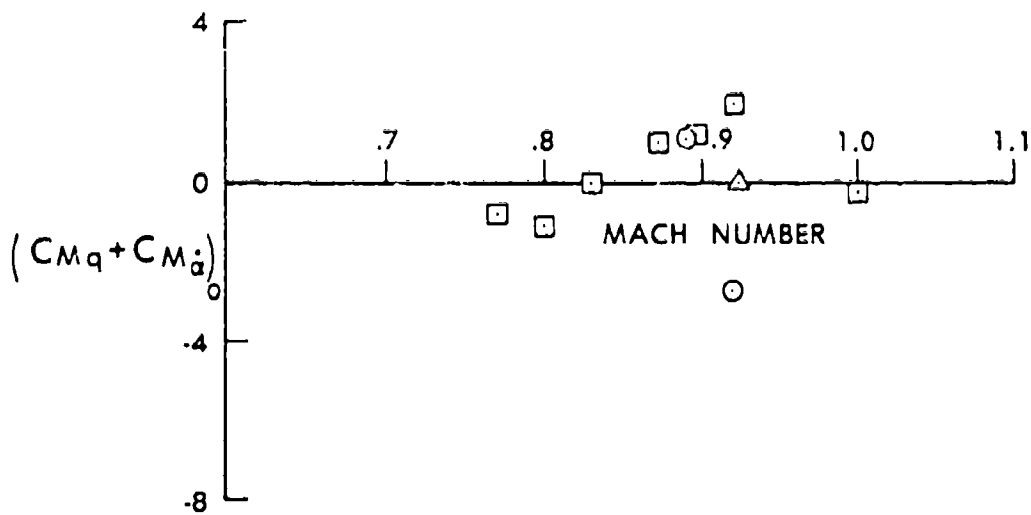


Figure 30. Pitch damping coefficient versus Mach number.

Wind Speed = 10 mph.
Range = 50 m.

Numbers correspond to wind
direction on a clock based
system.

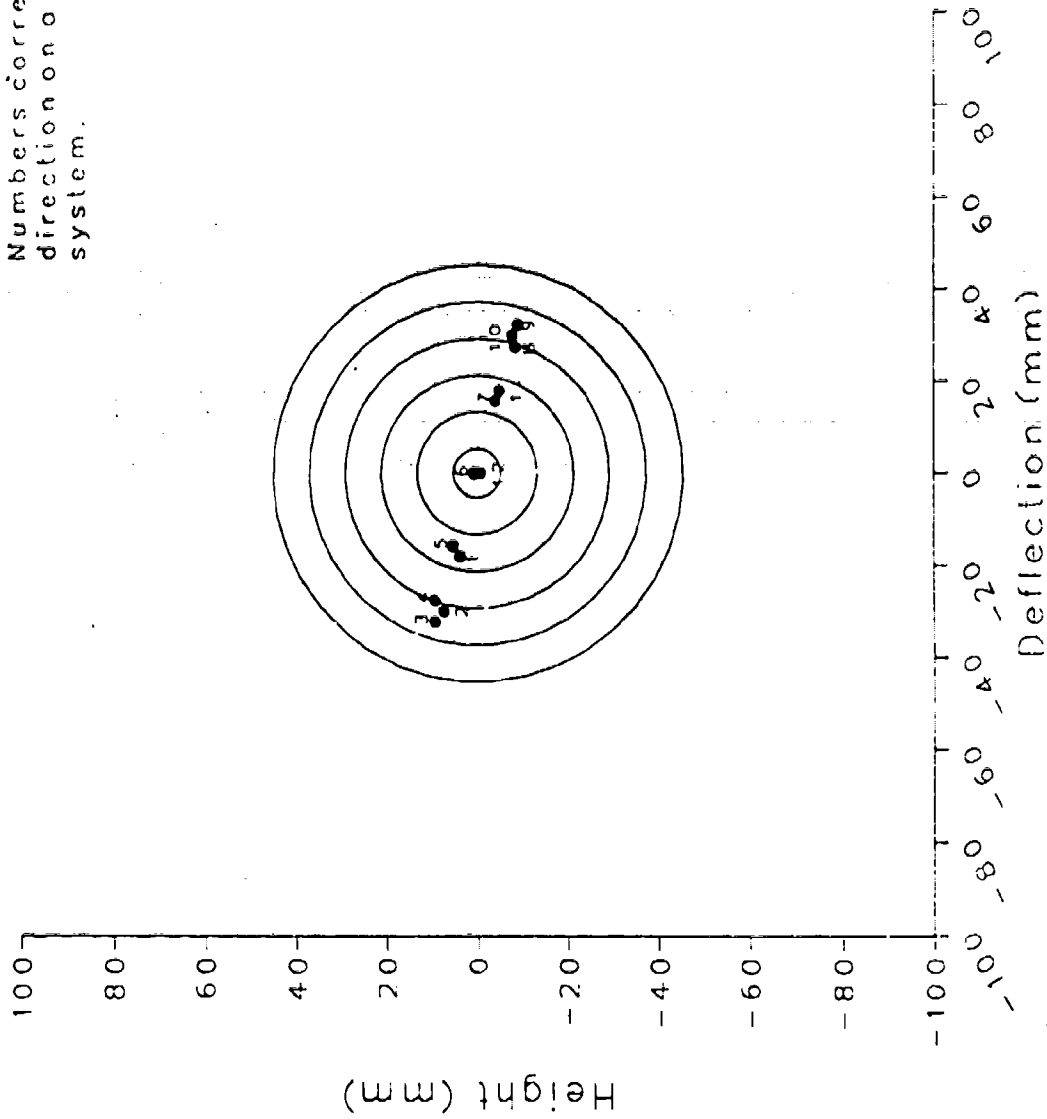


Figure 31. Effect of a 10 mile/hour wind on the Eley Tenex bullet at 50 metres range.

Wind Speed = 20 mph.
 Range = 50 m.

Numbers correspond to wind direction on a clock based system.

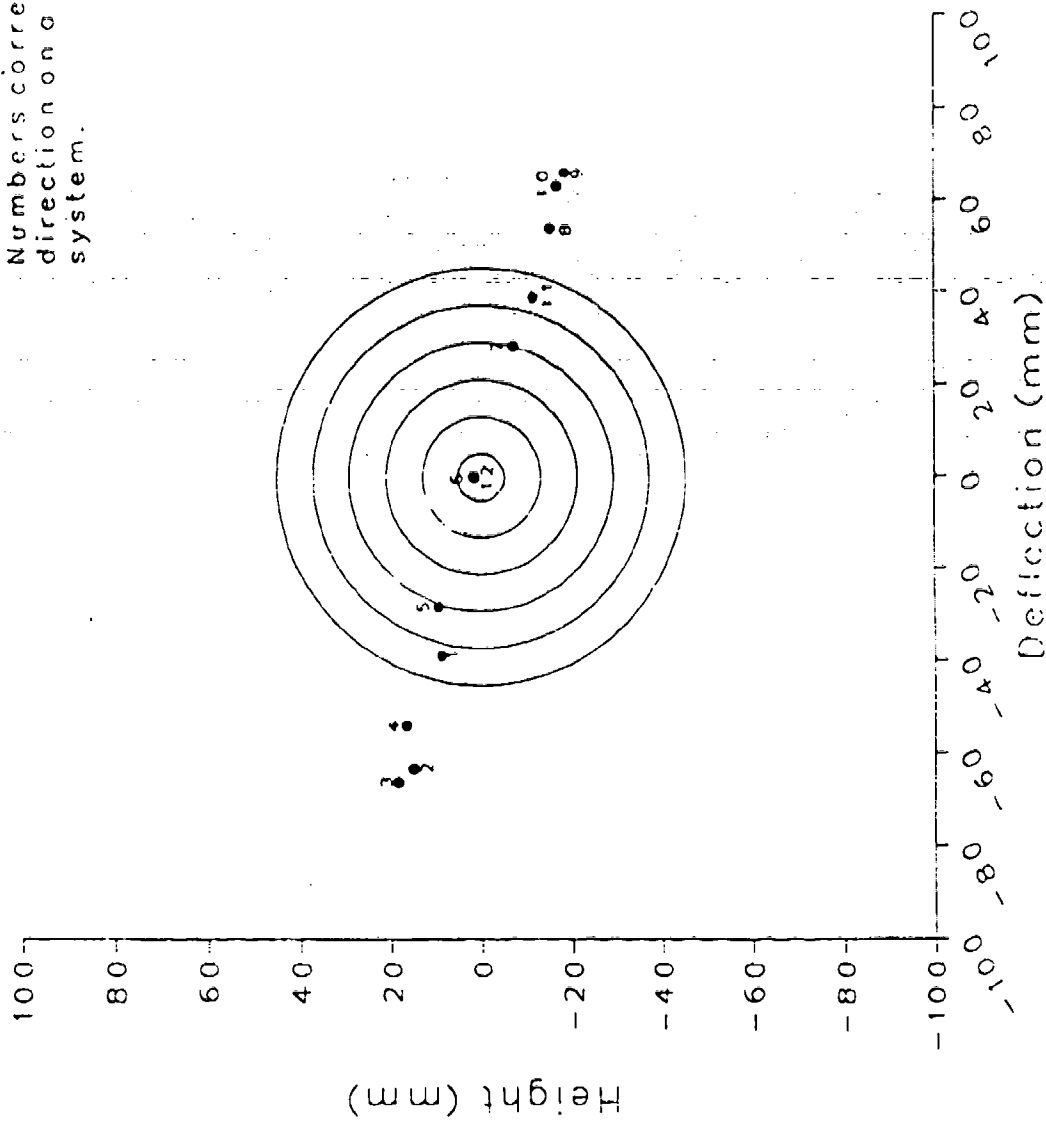


Figure 32. Effect of a 20 mile/hour wind on the Eley Tenex bullet at 50 metres range.

Wind Speed = 30 mph.
 Range = 50 m.

Numbers correspond to wind direction on a clock based system.

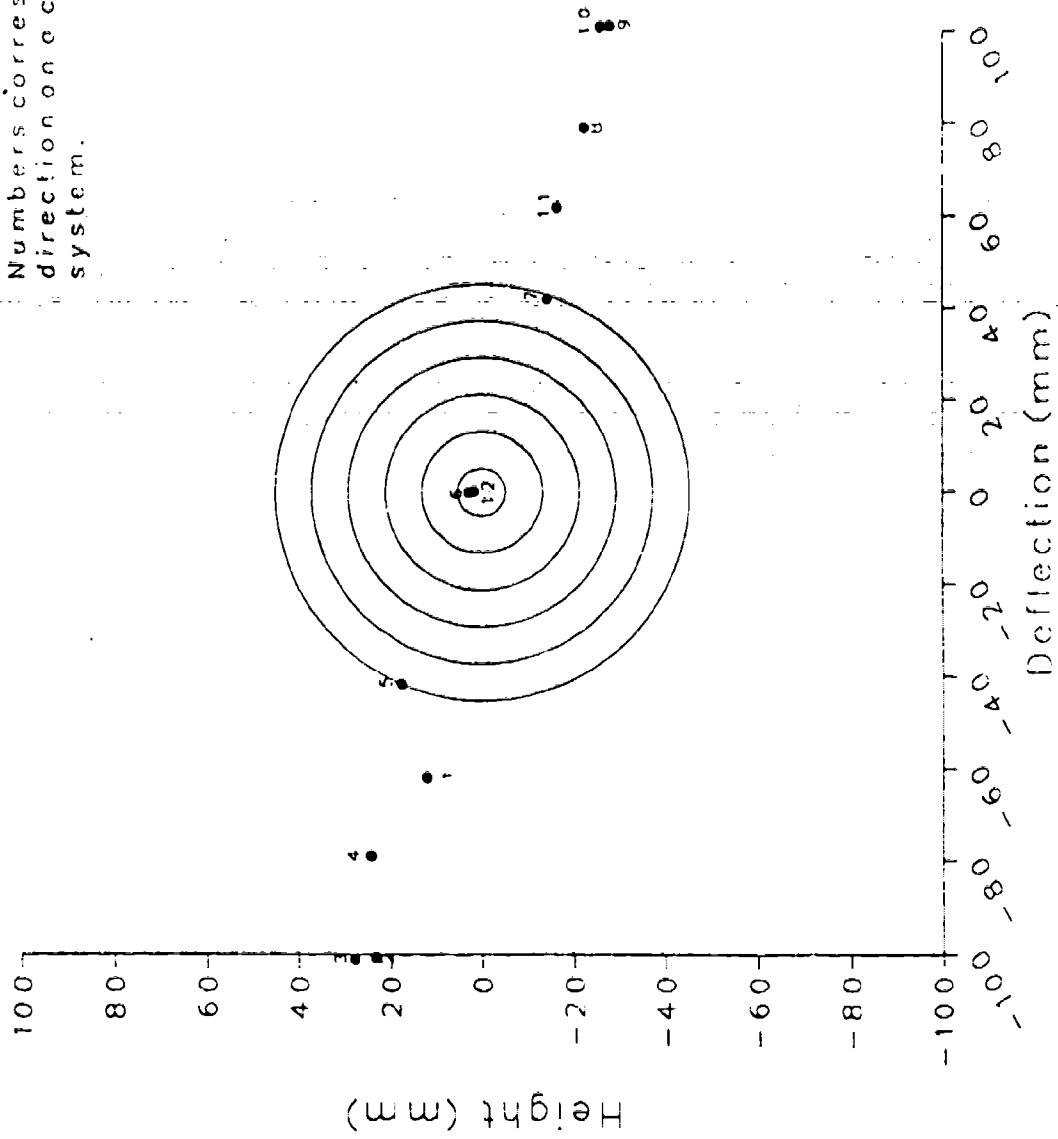


Figure 33. Effect of a 30 mile/hour wind on the Eley Tenex bullet at 50 metres range.

Wind Speed = 10 mph.
Range = 50 m.

Numbers correspond to wind direction on a clock based system.

Wind deflections calculated from Equations (11) and (12).

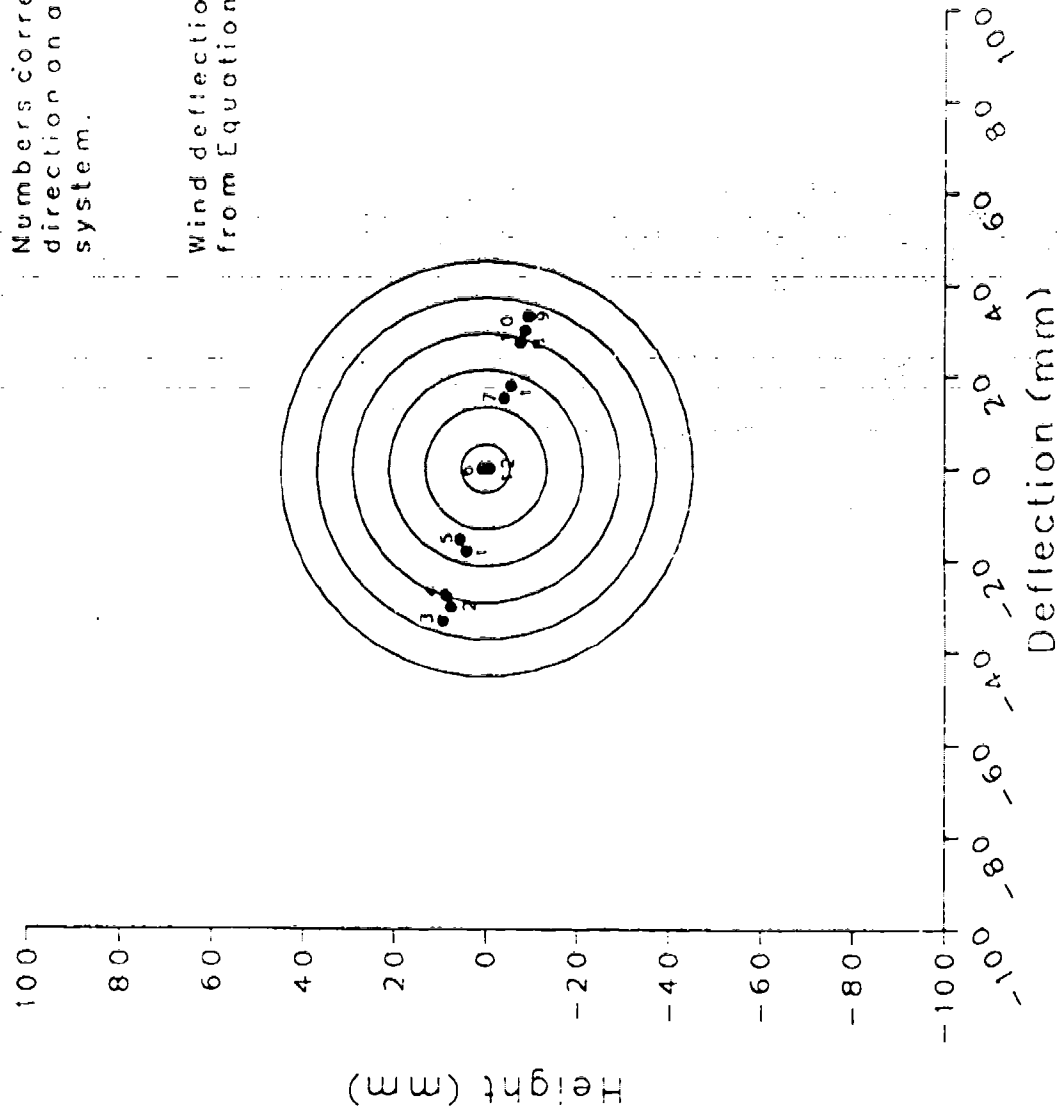


Figure 34. Simplified ballistic prediction of the wind effect on the Eley Tenex bullet at 50 metres range.

Table 1. Average Physical Characteristics of Caliber .22 Match Bullets.

Projectile	Reference Diameter (mm)	Weight (grams)	Center of Gravity (cal - base)	Axial Moment of Inertia (gm-cm ²)	Transverse Moment of Inertia (gm-cm ²)
Eley Tenex	5.69	2.59	.93	.0915	.269
RWS R-50	5.69	2.57	.95	.0894	.271
Eley Type Nose	5.69	2.60	.95	.0909	.291
Ultra Match	5.69	2.59	.94	.0928	.273

Table 2. Aerodynamic Characteristics of the Eley Tenex Bullet.

Round Number	Mach Number	α_i (degrees)	C_D	C_{M_x}	C_{L_x}	$C_{M_{y,z}}$	$(C_{M_x} + C_{M_y})$	C_{PN} (cal-base)
19266(a)	.945	.78	.304	--	--	--	--	--
19270(a)	.941	.61	.289	--	--	--	--	--
19271(a)	.936	.61	.275	1.46	--	--	--	--
19268(a)	.931	.62	.270	--	--	--	--	--
19269(a)	.930	.79	.276	--	--	--	--	--
19267(a)	.929	.38	.283	--	--	--	--	--
19280(a)*	.920	2.24	.275	1.25	2.33	.0	-4.7	1.41
19266(b)	.914	.41	.272	--	--	--	--	--
19270(b)	.913	.40	.260	--	--	--	--	--
19271(b)	.908	.58	.261	--	--	--	--	--
19268(b)	.901	.44	.256	--	--	--	--	--
19269(b)	.901	.73	.268	--	--	--	--	--
19267(b)	.900	.38	.266	--	--	--	--	--
19280(b)*	.891	2.11	.264	1.16	1.73	-.2	-1.5	1.51
19266(c)	.886	.43	.252	--	--	--	--	--
19270(c)	.886	3.64	.253	--	--	--	--	--
19271(c)	.881	3.73	.248	--	--	--	--	--
19268(c)	.875	.94	.243	--	--	--	--	--
19269(c)	.874	.20	.257	--	--	--	--	--
19267(c)	.873	.57	.251	--	--	--	--	--
19280(c)*	.865	2.13	.250	1.08	--	--	--	--

() Denotes Split Reduction
 * With Tipping Card Yaw Inducer

Table 3. Aerodynamic Characteristics of the RWS R-50 Bullet.

Round Number	Mach Number	α_i (degrees)	C_D	C_{M_x}	C_{L_x}	$C_{M_{y,z}}$	$(C_{M_y} + C_{M_z})$	CP_N (cal - base)
19286(a)	.941	.55	.297	--	--	--	--	--
19285(a)	.940	.53	.292	--	--	--	--	--
19286(b)	.911	.52	.269	--	--	--	--	--
19285(b)	.911	.50	.268	--	--	--	--	--
19286(c)	.884	.52	.250	--	--	--	--	--
19285(c)	.883	.53	.246	--	--	--	--	--

() Denotes Split Reduction
 * With Tipping Card Yaw Inducer

Table 4. Aerodynamic Characteristics of the Eley Type Nose Bullet.

Round Number	Mach Number	α_1 (degrees)	C_D	C_{M_x}	C_{L_x}	$C_{M_{y,z}}$	$(C_{M_x} + C_{M_{y,z}})$	CP_N (cal-base)
19275(a)	1.028	.38	.474	--	--	--	--	--
19282(a)*	1.000	2.85	.500	1.72	--	.0	-3.0	--
19275(b)	.976	.36	.377	--	--	--	--	--
19282(b)*	.953	3.49	.340	1.83	--	--	--	--
19272(a)	.944	1.56	.333	--	--	--	--	--
19275(c)	.941	4.54	.281	--	--	--	--	--
19281(a)*	.923	5.13	.351	1.48	1.84	.0	-3.1	1.62
19282(c)*	.919	4.04	.309	--	--	--	--	--
19272(b)	.911	1.76	.308	1.33	--	--	--	--
19274(a)	.895	1.24	.298	1.26	--	-.5	.8	--
19281(b)*	.885	4.69	.346	1.24	1.58	--	--	1.59
19272(c)	.879	1.97	.304	--	--	--	--	--
19273(a)	.873	1.42	.294	1.15	--	-.4	.9	--
19274(b)	.865	1.39	.290	--	--	--	--	--
19281(c)*	.861	4.52	.327	1.10	1.57	--	--	1.53
19273(b)	.844	1.60	.285	1.08	--	--	--	--
19274(c)	.838	1.50	.278	--	--	--	--	--
19283(a)*	.828	4.68	.316	1.11	1.96	-.3	.0	1.43
19273(c)	.817	1.64	.275	--	--	--	--	--
19283(b)*	.800	4.10	.297	1.07	2.04	-.1	-1.1	1.41
19283(c)*	.773	3.46	.284	1.07	2.38	-.1	-.8	1.35

() Denotes Split Reduction
 * With Tipping Card Yaw Inducer

Table 5. Aerodynamic Characteristics of the Ultra Match Bullet.

Round Number	Mach Number	α_i (degrees)	C_D	C_{M_x}	C_{L_x}	$C_{M_{y_0}}$	$(C_{M_{y_0}} + C_{M_{z_0}})$	CP_N (cal-base)
19276(a)	1.017	.55	.540	--	--	--	--	--
19276(b)	.962	.30	.372	--	--	--	--	--
19277(a)	.930	.83	.287	--	--	--	--	--
19276(c)	.929	.38	.280	--	--	--	--	--
19278(a)	.926	.27	.275	--	--	--	--	--
19284(a)*	.924	4.26	.321	1.49	2.31	.0	-5.2	1.51
19277(b)	.900	.97	.276	1.34	--	--	--	--
19278(b)	.898	.32	.265	--	--	--	--	--
19284(b)*	.890	4.06	.311	1.14	2.22	--	--	1.39
19277(c)	.872	.90	.265	--	--	--	--	--
19278(c)	.871	.20	.256	--	--	--	--	--
19284(c)*	.860	3.68	.291	1.02	2.41	--	--	1.32
19279(a)	.839	.74	.249	--	--	--	--	--
19279(b)	.815	1.07	.243	--	--	--	--	--
19279(c)	.792	.93	.237	--	--	--	--	--

() Denotes Split Reduction

* With Tipping Card Yaw Inducer

Table 6. Flight Motion Parameters of the Eley Tenex Bullet.

Round Number	Mach Number	S_y	S_d	$\lambda_F \times 10^3$ (1/cal)	$\lambda_S \times 10^3$ (1/cal)	K_F	K_S	ϕ'_F (r/cal)	ϕ'_S (r/cal)	Spin (r/cal)
19266(a)	.945	--	--	--	--	.0057	.0114	--	--	--
19270(a)	.941	--	--	--	--	.0041	.0091	--	--	--
19271(a)	.936	1.68	--	--	--	.0044	.0098	.0260	.0058	.0935
19268(a)	.931	--	--	--	--	.0061	.0088	--	--	--
19269(a)	.930	--	--	--	--	.0039	.0131	--	--	--
19267(a)	.929	--	--	--	--	.0032	.0057	--	--	--
19280(a)*	.920	1.83	.3	-.524	-.010	.0137	.0333	.0257	.0050	.0903
19266(b)	.914	--	--	--	--	.0038	.0049	--	--	--
19270(b)	.913	--	--	--	--	.0045	.0043	--	--	--
19271(b)	.908	--	--	--	--	.0044	.0082	--	--	--
19268(b)	.901	--	--	--	--	.0043	.0060	--	--	--
19269(b)	.901	--	--	--	--	.0027	.0111	--	--	--
19267(b)	.900	--	--	--	--	.0025	.0062	--	--	--
19280(b)*	.891	2.04	.1	-.231	.032	.0063	.0362	.0267	.0045	.0917
19266(c)	.886	--	--	--	--	.0050	.0049	--	--	--
19270(-)	.886	--	--	--	--	.0187	.0206	--	--	--
19271(c)	.881	--	--	--	--	.0248	.0268	--	--	--
19266(c)	.875	--	--	--	--	.0066	.0068	--	--	--
19269(c)	.874	--	--	--	--	.0031	.0006	--	--	--
19267(c)	.873	--	--	--	--	.0056	.0076	--	--	--
19280(c)*	.865	2.18	--	--	--	.0066	.0366	.0270	.0041	.0916

() Denotes Split Reduction

* With Tipping Card Yaw Inducer

Table 7. Flight Motion Parameters of the RWS R-50 Bullet.

Round Number	Mach Number	S_f	S_d	$\lambda_F \times 10^3$ (1/cal)	$\lambda_S \times 10^3$ (1/cal)	K_F	K_S	ϕ'_F (r/cal)	ϕ'_S (r/cal)	Spin (r/cal)
19286(a)	.941	--	--	--	--	.0073	.0059	--	--	--
19285(a)	.940	--	--	--	--	.0060	.0064	--	--	--
19286(b)	.911	--	--	--	--	.0068	.0060	--	--	--
19285(b)	.911	--	--	--	--	.0067	.0043	--	--	--
19286(c)	.884	--	--	--	--	.0059	.0067	--	--	--
19285(c)	.833	--	--	--	--	.0057	.0072	--	--	--

() Denotes Split Reduction
 * With Tipping Card yaw Inducer

Table 8. Flight Motion Parameters of the Eley Type Nose Bullet.

Round Number	Mach Number	S_f	S_d	$\lambda_F \times 10^3$ (1/cal)	$\lambda_S \times 10^3$ (1/cal)	K_F	K_S	ϕ'_F (r/cal)	ϕ'_S (r/cal)	Spin (r/cal)
19275(a)	1.028	--	--	--	--	.0034	.0034	--	--	--
19287(a)*	1.000	1.46	.3	-.606	.067	.0149	.0435	.0239	.0068	.0983
19275(b)	.976	--	--	--	--	.0032	.0051	--	--	--
19282(b)*	.953	1.48	--	--	--	.0057	.0599	--	--	--
19272(a)	.944	--	--	--	--	.0079	.0261	--	--	--
19275(c)	.941	--	--	--	--	.0202	.0358	--	--	--
19281(a)*	.923	1.48	.3	-.409	.013	.0282	.0821	.0277	.0062	.0925
19282(c)*	.919	--	--	--	--	.0032	.0702	--	--	--
19272(b)	.911	1.65	--	--	--	.0059	.0302	.0235	.0054	.0923
19274(a)	.895	1.58	--	-.146	.104	.0120	.0175	.0222	.0054	.0884
19281(b)*	.885	1.90	--	--	--	.0087	.0811	.0253	.0047	.0961
19272(c)	.879	--	--	--	--	.0037	.0341	--	--	--
19273(a)	.873	1.73	3.0	-.062	.076	.0170	.0179	.0227	.0048	.0882
19274(b)	.866	--	--	--	--	.0054	.0234	--	--	--
19281(c)*	.851	2.07	--	--	--	.0051	.0787	.0253	.0041	.0943
19273(b)	.844	1.93	--	--	--	.0127	.0243	.0238	.0043	.0902
19274(c)	.836	--	--	--	--	.0074	.0248	--	--	--
19283(a)*	.828	1.90	-.E	-.099	.029	.0526	.0611	.0236	.0044	.0904
19273(c)	.817	--	--	--	--	.0081	.0322	--	--	--
19283(b)*	.800	2.03	.3	-.168	-.004	.0319	.0625	.0246	.0041	.0920
19283(c)*	.773	2.15	.7	-.111	-.049	.0193	.0567	.0256	.0040	.0945

() Denotes Split Reduction

* With Tipping Card Yaw Inducer

Table 9. Flight Motion Parameters of the Ultra Match Bullet.

Round Number	Mach Number	S_g	S_d	$\lambda_F \times 10^3$ (1/cal)	$\lambda_S \times 10^3$ (1/cal)	K_F	K_S	ϕ'_F (r/cal)	ϕ'_S (r/cal)	Spin (r/cal)
19276(a)	1.017	--	--	--	--	.0043	.0066	--	--	--
19276(b)	.962	--	--	--	--	.0017	.0046	--	--	--
19277(a)	.930	--	--	--	--	.0032	.0141	--	--	--
19276(c)	.929	--	--	--	--	.0042	.0046	--	--	--
19278(a)	.926	--	--	--	--	.0023	.0037	--	--	--
19284(a)*	.924	1.67	.3	-.646	.028	.0191	.0669	.0260	.0058	.0935
19277(b)	.900	1.80	--	--	--	.0032	.0167	.0262	.0052	.0923
19278(b)	.898	--	--	--	--	.0000	.0054	--	--	--
19284(b)*	.890	2.05	--	--	--	.0086	.0699	.0264	.0044	.0906
19277(c)	.872	--	--	--	--	.0083	.0101	--	--	--
19278(c)	.871	--	--	--	--	.0013	.0031	--	--	--
19284(c)*	.860	2.01	--	--	--	.0161	.0579	.0246	.0042	.0848
19279(a)	.839	--	--	--	--	.0072	.0098	--	--	--
19279(b)	.815	--	--	--	--	.0082	.0167	--	--	--
19279(c)	.792	--	--	--	--	.0113	.0098	--	--	--

() Denotes Split Reduction
 * With Tipping Card Yaw Inducer

INTENTIONALLY LEFT BLANK.

References

1. Braun, W.F., "The Free Flight Aerodynamics Range," BRL Report No. 1048, U.S. Army Ballistic Research Laboratory, Aberdeen Proving Ground, Maryland, August 1958. (AD 202249)
2. Murphy C.H., "Data Reduction for the Free Flight Spark Ranges," BRL Report No. 900, U.S. Army Ballistic Research Laboratory, Aberdeen Proving Ground, Maryland, February 1954. (AD 35833)
3. Murphy, C.H., "The Measurement of Non-Linear Forces and Moments by Means of Free Flight Tests," BRL Report No. 974, U.S. Army Ballistic Research Laboratory, Aberdeen Proving Ground, Maryland, February 1956. (AD 93521)
4. McCoy, R. L., "Aerodynamic Characteristics of the 30mm, XM788 Projectile," BRL Memorandum Report No. 03019, U.S. Army Ballistic Research Laboratory, Aberdeen Proving Ground, Maryland, May 1980. (AD A086096)
5. Lieske, R. F. and McCoy, R. L., "Equations of Motion of a Rigid Projectile," BRL Report No. 1244, U.S. Army Ballistic Research Laboratory, Aberdeen Proving Ground, Maryland, March 1964. (AD 441598)
6. Murphy, C.H., "Free Flight Motion of Symmetric Missiles," BRL Report No. 1216, U.S. Army Ballistic Research Laboratory, Aberdeen Proving Ground, Maryland, July 1963. (AD 442757)

INTENTIONALLY LEFT BLANK.

List of Symbols

C_D	=	$\frac{\text{Drag Force}}{[(1/2)\rho V^2 S]}$	
C_{D_0}	=	zero-yaw drag coefficient	
$C_{D_{\delta^2}}$	=	quadratic yaw drag coefficient	
$C_{D_{\delta^4}}$	=	quartic yaw drag coefficient	
C_{L_α}	=	$\frac{\text{Lift Force}}{[(1/2)\rho V^2 S \delta]}$	<p>Positive coefficient: Force in plane of total angle of attack, α_t, \perp to trajectory in direction of α_t. (α_t directed from trajectory to missile axis.)</p> <p>$\delta = \sin \alpha_t$.</p>
C_{M_α}	=	$\frac{\text{Static Moment}}{[(1/2)\rho V^2 S d \delta]}$	<p>Positive coefficient: Moment increases angle of attack α_t.</p>
$C_{M_{p\alpha}}$	=	$\frac{\text{Magnus Moment}}{[(1/2)\rho V^2 S d (pd/V) \delta]}$	<p>Positive coefficient: Moment rotates nose \perp to plane of α_t in direction of spin.</p>
$C_{M_{p\alpha 0}}$	=	zero-yaw Magnus moment coefficient	
\tilde{C}_2	=	cubic Magnus moment coefficient	
C_{N_α}	=	$\frac{\text{Normal Force}}{[(1/2)\rho V^2 S \delta]}$	<p>Positive coefficient: Force in plane of total angle of attack, α_t, \perp to missile axis in direction of α_t. $C_{N_\alpha} \cong C_{L_\alpha} + C_D$</p>

List of Symbols (continued)

$$C_{N_{p\alpha}} = \frac{\text{Magnus Force}}{[(1/2)\rho V^2 S (pd/V) \delta]}$$

Negative coefficient: Force acts in direction of 90° rotation of the positive lift force against spin.

For most exterior ballistic uses, where $\dot{\alpha} \approx q$, $\dot{\beta} \approx -r$, the definition of the damping moment sum is equivalent to:

$$(C_{M_q} + C_{M_{\dot{\alpha}}}) = \frac{\text{Damping Moment}}{[(1/2)\rho V^2 S d (q, d/V)]}$$

Positive coefficient: Moment increases angular velocity.

$$(C_{M_q} + C_{M_{\dot{\alpha}}})_0 = \text{zero-yaw pitch damping moment coefficient}$$

$$C_{l_p} = \frac{\text{Roll Damping Moment}}{[(1/2)\rho V^2 S d (pd/V)]}$$

Negative coefficient: Moment decreases rotational velocity.

$$C_{P_N} = \text{center of pressure of the normal force, positive from base to nose}$$

$$c.m. = \text{center of mass}$$

$$d = \text{body diameter of projectile, reference length}$$

$$d_2 = \text{cubic pitch damping moment coefficient}$$

$$I_x = \text{axial moment of inertia}$$

$$I_y = \text{transverse moment of inertia}$$

$$K_F, K_1 = \text{magnitude of the fast yaw mode}$$

$$K_S, K_2 = \text{magnitude of the slow yaw mode}$$

$$l = \text{length of projectile}$$

$$m = \text{mass of projectile}$$

$$M = \text{Mach number}$$

List of Symbols (continued)

p	=	roll rate	
q, r	=	transverse angular velocities	
q_t	=	$(q^2 + r^2)^{\frac{1}{2}}$	
R	=	subscript denotes range value	Example: $[C_D]_R$ is the coefficient value measured in a free-flight spark photography range facility for total drag.
s	=	dimensionless arc length along the trajectory	
S	=	$(\pi d^2/4)$, reference area	
S_d	=	dynamic stability factor	
S_g	=	gyroscopic stability factor	
V	=	velocity of projectile	
α, β	=	angle of attack, side slip	
α_t	=	$(\alpha^2 + \beta^2)^{\frac{1}{2}} = \sin^{-1} \delta$, total angle of attack	
λ_F, λ_1	=	fast mode damping rate	negative λ indicates damping
λ_S, λ_2	=	slow mode damping rate	negative λ indicates damping
ρ	=	air density	
ϕ'_F, ϕ'_1	=	fast mode frequency	
ϕ'_S, ϕ'_2	=	slow mode frequency	

List of Symbols (continued)

Effective Squared Yaw Parameters

$$\bar{\delta} \cong K_F^2 + K_S^2$$

$$\delta_{eF}^2 = K_F^2 + 2K_S^2$$

$$\delta_{eS}^2 = 2K_F^2 + K_S^2$$

$$\delta_{eTT}^2, \delta_e^2 = K_F^2 + K_S^2 + \frac{(\phi'_F K_F^2 - \phi'_S K_S^2)}{(\phi'_F - \phi'_S)}$$

$$\delta_{eHH}^2 = \left(\frac{I_y}{I_x} \right) \left[\frac{(\phi'_F + \phi'_S) (K_S^2 - K_F^2)}{(\phi'_F - \phi'_S)} \right]$$

$$\delta_{eTH}^2 = \left(\frac{I_x}{I_y} \right) \left[\frac{(K_F^2 \phi_F'^2 - K_S^2 \phi_S'^2)}{(\phi_F'^2 - \phi_S'^2)} \right]$$

$$\delta_{eHT}^2 = \frac{(\phi'_F K_S^2 - \phi'_S K_F^2)}{(\phi'_F - \phi'_S)}$$

No of Copies	Organization	No of Copies	Organization
2	Administrator Defense Technical Info Center ATTN: DTIC-DDA Cameron Station Alexandria, VA 22304-6145	1	Director US Army Aviation Research and Technology Activity ATTN: SAVRT-R (Library) M/S 219-3 Ames Research Center Moffett Field, CA 94035-1000
1	HQDA (SARD-TR) WASH DC 20310-0001	1	Commander US Army Missile Command ATTN: AMSMI-RD-CS-R (DOC) Redstone Arsenal, AL 35898-5010
1	Commander US Army Materiel Command ATTN: AMCDRA-ST 5001 Eisenhower Avenue Alexandria, VA 22333-0001	1	Commander US Army Tank-Automotive Command ATTN: AMSTA-TSL (Technical Library) Warren, MI 48397-5000
1	Commander US Army Laboratory Command ATTN: AMSLC-DL Adelphi, MD 20783-1145	1	Director US Army TRADOC Analysis Command ATTN: ATRC-WSR White Sands Missile Range, NM 88002-5502
2	Commander US Army, ARDEC ATTN: SMCAR-JMI-1 Picatinny Arsenal, NJ 07806-5000	(Class. only) 1	Commandant US Army Infantry School ATTN: ATSH-CD (Security Mgr.) Fort Benning, GA 31905-5660
2	Commander US Army, ARDEC ATTN: SMCAR-TDC Picatinny Arsenal, NJ 07806-5000	(Unclass. only) 1	Commandant US Army Infantry School ATTN: ATSH-CD-CSO-OR Fort Benning, GA 31905-5660
1	Director Benet Weapons Laboratory US Army, ARDEC ATTN: SMCAR-CCB-TL Watervliet, NY 12189-4050	1	Air Force Armament Laboratory ATTN: AFATL/DLODL Eglin AFB, FL 32542-5000
1	Commander US Army Armament, Munitions and Chemical Command ATTN: SMCAR-ESP-L Rock Island, IL 61299-5000		<u>Aberdeen Proving Ground</u>
1	Commander US Army Aviation Systems Command ATTN: AMSAV-DACL 4300 Goodfellow Blvd. St. Louis, MO 63120-1798	2	Dir, USAMSAA ATTN: AMXSY-D AMXSY-MP, H. Cohen
		1	Cdr, USATECOM ATTN: AMSTE-TD
		3	Cdr, CRDEC, AMCCOM ATTN: SMCCR-RSP-A SMCCR-MU SMCCR-MSI
		1	Dir, VLAMO ATTN: AMSLC-VL-D

<u>No. of Copies</u>	<u>Organization</u>	<u>No. of Copies</u>	<u>Organization</u>
2	Air Force Armament Laboratory ATTN: AFATL/FXA, Mr. G. Abate Mr. G. Winchenbach Eglin AFB, FL 32542-5000	1	Commanding General MCDEC ATTN: Code D091 Fire Power Division Quantico, VA 22134-5080
1	Director HQ, TRAC RPD ATTN: ATRC-RP Fort Monroe, VA 23651-5143	2	Commandant US Army Air Defense Artillery School ATTN: ATSA-CDM-W, CPT Taylor ATSA-CDE, Mr. J. Abston Fl. Bliss, TX 79916-7050
1	Commander TRAC-FLVN ATTN: ATRC Fort Leavenworth, KS 66027-5200	1	National Rifle Association ATTN: Mr. Gary L. Anderson Executive Director NRA-GO 1600 Rhode Island Avenue, NW Washington, DC 20036
1	Director TRAC-WSMR White Sands Missile Range, NM 88002-5502	1	Shooting Sports USOTC ATTN: Mr. Tim Conrad 1750 East Boulder Street Colorado Springs, CO 80909
1	Commander HQ AMCCOM ATTN: AMSMC-ASA-A, Mr. L. Niebuhr Rock Island, IL 61299-6000	1	NRA Publications ATTN: Mr. Pete Dickey American Rifleman Technical Editor 470 Spring Park Place Suite 1000 Herndon, VA 22070
1	President US Army Infantry Board ATTN: ATZB-IB-SA, Mr. L. Tomlinson Fort Benning, GA 31905-5800	1	JJRTC ATTN: Mr. Carl Flowers Powder Mill Drive, R-2 Laurel, MD 20707
1	Commander Naval Sea Systems Command ATTN: Code 62CE, Mr. R. Brown Washington, DC 20362-5101	1	MTU WTB MCCDC ATTN: Mr. Dennis Ghiselli Quantico, VA 22134
4	Commanding Officer Naval Weapons Support Center ATTN: Code 2021, Bldg. 2521, Mr. C. Zeller Code 2022, Mr. R. Henry Mr. G. Dornick Dr. J. Maassen Crane, IN 47522-5020	1	Shooting Sports USOTC ATTN: Mr. Dan Iuga National Pistol Coach 1750 East Boulder Street Colorado Springs, CO 80909
		1	USAMU ATTN: Mr. Bill Krilling Fl. Benning, GA 31905

<u>No. of Copies</u>	<u>Organization</u>
4	Shooting Sports USOTC. ATTN: Mr. Robert K. Mitchell National Rifle Coach 1750 East Boulder Street Colorado Springs, CO 80909
1	MTU WTB MCCDC ATTN: MAJ O'Connell Quantico, VA 22134
1	U.S. Olympic Training Center Sports Medicine Building ATTN: Mr. Tom Westenberg 1750 East Boulder Street Colorado Springs, CO 80909
1	Shooting Sports USOTC ATTN: Mr. Lones Wigger, Jr. National Shooting Team Director 1750 East Boulder Street Colorado Springs, CO 80909
1	Tioga Engineering Company ATTN: Mr. W. Davis, Jr. 13 Cone Street Wellsboro, PA 16901
1	Dr. Henry D. Cross, III 216 Heyer's Mill Road Colts Neck, NJ 07722
1	Ms. Marsha Beasley 1301 Van Voorhis Road, Apt. L Morgantown, WV 26505
1	Mr. Joe Berry P.O. Box 1454 Nevada City, CA 95959
1	Mr. Ray Carter 1230 Sixteenth Street, NW Washington, DC 20036
1	Mr. Steve Chernicky 6731 Via de la Reina Bonsall, CA 92003

<u>No. of Copies</u>	<u>Organization</u>
1	Dr. Wendell Fairbanks 2021 Box Butte Alliance, NB 69301
1	Dr. Craig Farnsworth 155 South Wadsworth Suite 1 Denver, CO 80226
1	Mr. A. P. Ferrante 307 Joseph Street Greenville, NC 27858
1	Mr. Gene Harwood 561 West Street St. Helens, OR 97051
1	Mr. Neal Johnson 111 Marvin Drive Hampton, VA 23666-2636
1	Mr. Dick Newman 11 Knollwood Drive Cherry Hill, NJ 08002
1	Mr. William C. Pullum 507 Candlewood Drive Enterprise, AL 36330
1	Mr. Don Rummier 315 Rapidan Road Hampton, VA 23669

<u>No. of Copies</u>	<u>Organization</u>
16	Commander US Army, ARDEC ATTN: SMCAR-AET-AP, Mr. R. Kline SMCAR-CCL-AD, Mr. F. Puzycki Mr. W. Schupp Mr. R. Mazeski Mr. D. Conway SMCAR-CCL-C SMCAR-CCL-FA, Mr. R. Schlenner Mr. J. Fedewitz Mr. P. Wyluda SMCAR-FSF-GD, Mr. K. Pflieger SMCAR-CCL-SP, Mr. W. Bunting Mr. P. Errante SMCAR-CCJ, Mr. J. Ackley Mr. V. Shisler Mr. H. Wreden Mr. J. Hill Picatinny Arsenal, NJ 07806-5000

Aberdeen Proving Ground

5	Director, USAMSAA ATTN: AMXSY-J, Mr. K. Jones Mr. M. Carroll Mr. J. Weaver Mr. E. Heiss AMXSY-GI, Mr. L. DeLattre
1	Commander, USATECOM ATTN: AMSTE-SI-F
2	Commander, CRDEC, AMCCOM ATTN: SMCCR-RSP-A, Mr. M. Miller Mr. J. Huerta
3	Director, USAHEL ATTN: SLCHE-IS, Mr. B. Corona Mr. P. Ellis Mr. J. Torre

<u>No. of Copies</u>	<u>Organization</u>
1	Director, USACSTA ATTN: STECS-AS-LA, Mr. G. Niewenhaus

USER EVALUATION SHEET/CHANGE OF ADDRESS

This Laboratory undertakes a continuing effort to improve the quality of the reports it publishes. Your comments/answers to the items/questions below will aid us in our efforts.

1. BRL Report Number BRL-MR-3877 Date of Report NOVEMBER 1990
2. Date Report Received _____
3. Does this report satisfy a need? (Comment on purpose, related project, or other area of interest for which the report will be used.) _____

4. Specifically, how is the report being used? (Information source, design data, procedure, source of ideas, etc.) _____

5. Has the information in this report led to any quantitative savings as far as man-hours or dollars saved, operating costs avoided, or efficiencies achieved, etc? If so, please elaborate. _____

6. General Comments. What do you think should be changed to improve future reports? (Indicate changes to organization, technical content, format, etc.) _____

CURRENT
ADDRESS

Name

Organization

Address

City, State, Zip Code

7. If indicating a Change of Address or Address Correction, please provide the New or Correct Address in Block 6 above and the Old or Incorrect address below.

OLD
ADDRESS

Name

Organization

Address

City, State, Zip Code

(Remove this sheet, fold as indicated, staple or tape closed, and mail.)

-----FOLD HERE-----

DEPARTMENT OF THE ARMY

Director
U.S. Army Ballistic Research Laboratory
ATTN: SLCBR-DD-T
Aberdeen Proving Ground, MD 21005-5066

OFFICIAL BUSINESS



**NO POSTAGE
NECESSARY
IF MAILED
IN THE
UNITED STATES**

BUSINESS REPLY MAIL
FIRST CLASS PERMIT No 0001, APG, MD

POSTAGE WILL BE PAID BY ADDRESSEE

Director
U.S. Army Ballistic Research Laboratory
ATTN: SLCBR-DD-T
Aberdeen Proving Ground, MD 21005-9989

-----FOLD HERE-----

